Title: A view of the pan-genome of domesticated cowpea (*Vigna unguiculata* [L.] Walp.)

Authors:

Qihua Liang, María Muñoz-Amatriaín, Shengqiang Shu, Sassoum Lo, Xinyi Wu, Joseph W. Carlson, Patrick Davidson, David M. Goodstein, Jeremy Phillips, Nadia M. Janis, Elaine J. Lee, Chenxi Liang, Peter L. Morrell, Andrew D. Farmer, Pei Xu, Timothy J. Close, Stefano Lonardi

Author contributions: Biological materials (SaL, XW, PX, MMA, TJC), Assembly (StL), SNP and structural variant calling (QL), Gene Annotation (SS), CowpeaPan (JWC, PD, DMG, JP), GO enrichment analysis (MMA, ADF), VeP annotation and gene size comparisons (NMJ, EJL, CL, PLM), synteny view (ADF), manuscript preparation (TJC, StL, MMA, QL, PLM, AF)

Keywords: Cowpea, *Vigna unguiculata*, pan-genome, genetic variation, SNPs, presence/absence variants (PAV), inversions, IT97K-499-35, Suvita-2, Sanzi, CB5-2, UCR779, TZ30, ZN016

Abstract:

Cowpea, *Vigna unguiculata L.* Walp., is a diploid warm-season legume of critical importance as both food and fodder in sub-Saharan Africa. This species is also grown in Northern Africa, Europe, Latin America, North America and East/Southeast Asia. To capture the genomic diversity of domesticates of this important legume, *de novo* genome assemblies were produced for representatives of six sub-populations of cultivated cowpea identified previously from genotyping of several hundred diverse accessions. A total of 44,861 genes were identified in the resulting pan-genome, including 21,330 core and 23,531 non-core genes. Therefore, the total number of genes in the domesticated cowpea pan-genome is more than double the number of genes in any of the individual genomes. GO-Terms associated with response to stress, defense response in particular, were highly enriched among the non-core genes, while core genes were significantly enriched in terms associated with catabolic processes, transport and cellular homeostasis, among others. Over 5 million SNPs relative to each individual assembly and over 40 structural variants >1 Mb in size were identified by comparing genomes. Vu10 was the chromosome with the highest frequency of SNPs and Vu04 had the most structural variants of all sizes. While similar numbers of synonymous SNPs and in-frame indels were found in core and non-core genes, non-core genes had much higher numbers of missense, stop gain, and frameshift mutations. These results suggest that non-core genes make a large contribution to diversity within domesticated cowpeas, and may be particularly important in terms of the contribution of large-effect variants.

Title: A view of the pan-genome of domesticated cowpea (*Vigna unguiculata* [L.] Walp.)

Article Summary (80 words maximum)

This study reports annotated genome assemblies of six cowpea accessions. Together with the previously reported annotated genome of IT97K-499-35, these constitute a pan-genome resource representing six subpopulations of domesticated cowpea. Annotations include genes, variant calls for SNPs and short indels, larger presence/absence variants and inversions. Non-core genes are enriched for loci involved in stress response and harbor the majority of genic variants with potential effects on coding sequence.

Introduction:

Individuals within a species vary in their genomic composition. The genome of any individual does not include the full complement of genes contained within the species. A pan-genome includes genes that are core to the species (shared among all individuals) and those absent from one or more individuals (non-core, dispensable, or variable genes). This pan-genome concept started to be applied to plants by Morgante *et al*. (2007) but began in bacterial species (reviewed by Golicz *et al.* 2020). Due to the complexity of plant genomes, the first studies exploring gene presence-absence variation (PAV) in plants used reduced-representation approaches, including array comparative genomic hybridization (CGH) and sequencing of transcriptomes (e.g. Springer *et al.* 2009, Muñoz-Amatriaín *et al.* 2013; Hirsch *et al.* 2014). Once sequencing of entire plant genomes became feasible, several pan-genomes of variable degrees of completeness were generated, and it was soon understood that PAV is prevalent in plants and that the pan-genome of any plant species is larger than the genome of any individual accession (reviewed by Lei *et al.* 2021). Moreover, many of the genes not present in reference accessions have functions of potential adaptive or agronomic importance such as time to flowering, and response to abiotic and biotic stresses (Gordon *et al.* 2017; Montenegro *et al.* 2017; Bayer *et al*. 2020), making the construction of a pan-genome a crucial task for those crops of global importance.

Cowpea is a diploid (2n = 22) member of the family Fabaceae tribe Phaseoleae, closely related to mung bean, common bean, soybean, and several other warm-season legumes. Cowpea was domesticated in Africa, but its cultivation has spread throughout most of the globe (Herniter *et al*., 2020). The inherent resilience of the species to drought and high temperatures (Hall 2004), together with its nutritional value as a reliable source of plant-based protein and folic acid, position cowpea favorably as a component of sustainable agriculture in the context of global climate change. Most cowpea production and consumption presently occur in sub-Saharan Africa, especially in the Sudano-Sahelian Zone with production mainly by smallholder farmers, often as an intercrop with maize, sorghum, or millet (Boukar *et al*., 2019). Tender green seeds are often consumed during the growing season, and immature pods are eaten as a vegetable,

especially in East and Southeast Asia. In addition, fresh leaves are sometimes consumed. The dry haulms are harvested and sold as fodder for livestock. Spreading varieties are also utilized as cover crops to prevent soil erosion and for weed control.

A reference genome sequence of cowpea cv. IT97K-499-35 was previously generated (Lonardi *et al*., 2019). Preliminary sequence comparisons using whole genome shotgun (WGS) data of 36 accessions suggested that extensive SNP and structural variation exists within domesticated cowpea (Lonardi *et al*., 2019). Cowpea also displays a wide range of phenotypic variation, and genetic assignment approaches have identified six subpopulations within cultivated cowpea germplasm (Muñoz-Amatriaín *et al*., 2021). These observations support the need to develop cowpea pan-genome resources based on a diverse set of cowpea accessions.

This study reports *de novo* assemblies of six cowpea accessions. Each accession was annotated using transcriptome sequences from the accession along with *ab initio* methods. These genome sequences, together with the previously reported sequence of IT97K-499-45 (Lonardi *et al*., 2019), constitute a pan-genome resource for domesticated cowpea. Using annotations for the seven genomes including genes, along with variant calls for SNPs and short indels, and larger structural variants, the following questions were addressed: (i) What proportion of genes are core and non-core, and do core and noncore genes differ in size or functional class? (ii) What proportion of large-effect mutations are created by single nucleotide variants versus structural variants (including indels), and do the proportions of large-effect variants differ among core and noncore genes? (iii) To what extent are gene content and gene order consistent across accessions within the species *V. unguiculata* and across species within the genus *Vigna* and the tribe Phaseoleae? The results suggest that both extensive structure differences among individual accession and the nature of variation in non-core genes are important considerations in efforts to identify genetic variation with adaptive potential.

Materials & Methods:

Cowpea accessions selected for sequencing (Supplemental Table S01)

Accessions chosen for sequencing and *de novo* assembly represented the six subpopulations of domesticated cowpea described in Muñoz-Amatriaín et al. (2021), as indicated in Figure 1. The intention of choosing accessions that cover each subpopulation was to maximize the discovery of genetic variations relevant to cultivated cowpea using a small number of samples. As shown by Gordon *et al.* (2017) in *Brachypodium distachyon*, the addition of individuals from subpopulations not previously sampled contributes much more to increasing the size of the pan-genome than the addition of individuals that are closely related.

IT97K-499-35 is a blackeye variety with resistance to the parasitic plants Striga and Alectra, developed at the International Institute of Tropical Agriculture in Ibadan, Nigeria (Singh *et al*., 2006) and provided by Michael Timko (U Virginia, Charlottesville, Virginia, USA) to the University of California Riverside (UCR) in 2006. The sequence assembly and annotation of IT97K-499-35 were described in Lonardi et al. (2019). CB5-2 is a fully inbred isolate that is closely related to CB5, which was the predominant Blackeye of the US Southwest for several decades. CB5 (Blackeye 8415) was bred by WW Mackie at the University of California (Mackie, 1946) to add resistances to Fusarium wilt and nematodes to a California Blackeye landrace, and provided to UCR by K Foster, University of California, Davis, in 1981. Suvita-2, also known as Gorom Local (IITA accession TVu-15553, US NPGR PI 583259), is somewhat resistant to bruchids and certain races of Striga, and is relatively drought tolerant. This landrace was collected from a local market by VD Aggarwal at the Institut de l'Environnement et de Recherches Agricoles (INERA) in Burkina Faso (Aggarwal *et al*.,1984) and provided to UCR by VD Aggarwal in 1983. Sanzi is an early flowering, small-seeded landrace from Ghana with resistance to flower bud thrips (Boukar *et al*., 2013), provided by KO Marfo, Nyankpala Agricultural Experiment Station, Tamale, Ghana to UCR in 1988. UCR779 (PI 583014) is a landrace from Botswana (de Mooy, 1985; Ehlers et al., 2002) that was provided to UCR as B019-A in 1987 by CJ de Mooy of Colorado State University. Yardlong bean or asparagus bean (cv.-gr. Sesquipedalis), the vegetable type of cowpea, is widely grown in Asian countries for consumption of tender long pods. TZ30 is an elite Chinese variety with the pod length of around 60 cm. ZN016 is a landrace originating from southeastern China with the pod length of around 35 cm and showing resistances to multiple major diseases of cowpea. TZ30 and ZN016 were used previously as parents of a mapping population to study the inheritance of pod length (Xu *et al*., 2017).

DNA sequencing and *de novo* assembly of seven cowpea accessions

The annotated genome (v1.0) of African variety IT97K-499-35 was assembled from Pacific Biosciences (Menlo Park, California, USA) long reads, two Bionano Genomics (San Diego, California, USA) optical maps and ten genetic linkage maps as described previously (Lonardi *et al*., 2019). The six additional *de novo* assemblies were produced by Dovetail Genomics (Scotts Valley, California, USA) using Illumina (San Diego, California, USA) short reads (150x2). DNA was extracted by Dovetail Genomics from seedling tissue of CB5-2, TZ30 and ZN016, and from seeds of CB5-2, Suvita-2, Sanzi and UCR779. Meraculous (Chapman *et al*., 2011) was used to assemble the reads, then sequences from Dovetail Chicago® and Dovetail Hi-C® libraries were added (using their proprietary pipeline) to resolve misassemblies and increase contiguity. These assemblies were then further refined using ALLMAPS (Tang *et al*., 2015). This analysis used ten previously reported genetic linkage maps to relate assemblies to the standard orientations and

numbering of the eleven cowpea chromosomes, as described in Lonardi *et al*. (2019) for IT97K-499-35. See "Data Availability Statement" for access to raw data and assemblies.

Calling of SNPs, indels, and structural variants

SNPs and indels were called using each reference genome versus the reads from the six other accessions. Reads of each accession described above for genome assemblies, plus short-read sequences produced by 10X Genomics from IT97K-49-35, were mapped to all assemblies using BWA (Li *et al.*, 2009). SNPs and indels were called using the GATK 4.2.0 pipeline in GVCF mode for each accession. All the per-sample GVCFs were gathered in joint genotyping to produce a set of joint-called SNPs and indels. Both per-sample SNPs and joint-called SNPs were filtered with same parameters of 'QD < 2.0 || FS > 60.0 || MQ < 40.0 || MQRankSum < -12.5 || ReadPosRankSum < -8.0 || SOR > 4.0'. Indels were filtered with 'QD < 2.0 || FS > 200.0 || ReadPosRankSum < -20.0 || SOR > 10.0'.

Each pair of individual genomes was aligned using minimap2 (Li, 2018), producing $\binom{7}{2} = 21$ alignment files. Structural variants including inversions and translocations were identified from the alignment files using SyRI (Goel *et al*., 2019). Figures were produced using PlotSR (Goel *et al*., 2022). Depth analyses were carried out using Mosdepth (Pedersen & Quinlan 2018). The average nucleotide diversity within and between populations was calculated from a VCF file using Pixy (Korunes *et al*., 2021).

Annotation of genes and repeats

All genomes were annotated using the JGI plant genome annotation pipelines (Shu *et al.*, 2014) integrated gene call (IGC), and gene model improvement (GMI). Both IGC and GMI are evidence-based gene call pipelines. In IGC, a gene locus was defined by peptide alignments of related organism homologous peptides and with alignments of within-organism transcriptome assemblies. Genes were predicted by homology-based gene prediction programs FGENESH+ (Salamov and Solovyev, 2000), FGENESH_EST and GenomeScan (Yeh *et al.*, 2001), and a JGI in-house homology-constrained transcriptome assembly ORF finder. Homologous proteomes included *Arabidopsis thaliana* and those from common bean (*Phaseolus vulgaris*), soybean (*Glycine max*), barrel medic (*Medicago truncatula*), poplar (*Populus trichocarpa*), rice (*Oryza sativa*), grape (*Vitis vinifera*) and Swiss-Prot. For transcript-based annotations of the six new assemblies, RNA for RNA-seq was extracted using Qiagen RNeasy Plant (Hilden, Germany) from each accession from well-hydrated and drought-stressed young seedling root and leaves, young flower buds, and pods five days after pollination, and from developing seeds of Suvita-2, TZ30 and ZN016 (not CB5-2, Sanzi or UCR779) 13 days after pollination. RNA quality was

assessed and concentrations were determined using an Agilent 2100 BioAnalyzer (Santa Clara, California, USA) and the Agilent RNA 6000 Nano Kit. The RNA-seq short reads from each accession were assembled using a JGI in-house genome-guided assembler, PERTRAN (Shu *et al*., 2013), using each genome assembly. Each short-read-based assembly and UNIGENE sequences (P12_UNIGENES.fa from harvest.ucr.edu) were fed into PASA (Haas *et al*., 2003) to produce transcriptome assemblies. A best gene per locus (based on evidence) was defined using PASA from PASA alignment of transcriptome assemblies for splicing correctness, alternative transcripts, and UTR addition. The PASA genes were filtered to obtain the final gene set, including an automated repeat coding sequence (CDS) overlap filter, a manual low-quality gene filter, and an automatic filter from transposable element (TE) protein domain assignments. This process was repeated once with one additional homology seeding of non-self, high-confidence gene models.

Determination of core and non-core genes among seven accessions

Coding sequences (CDS) of genes in IT97K-499-35 were mapped to CDS from the other six accessions using BLAT (Kent, 2002). Alignments with 95% identity and 90% length coverage were counted as positive matches. One-to-one alignments were immediately recorded, while one-to-many alignments were resolved as follows. If a gene A mapped to a set of genes $B_1,\ldots,B_n$, gene A was assigned to the gene B_i that shared the most one-to-one neighboring genes with A. After finding the correspondences between IT97K-499-35 genes to genes from the other accessions, the same strategy was repeated to seek correspondences for unpaired genes from CB5-2 by mapping to unpaired genes from remaining five accessions, and so on in the order of Suvita-2, Sanzi, UCR779, ZN016 and TZ30. The seven assemblies were aligned using progressiveMauve (Darling *et al*., 2010), to identify core genomic blocks using a pan-genome representation called PGV (Liang and Lonardi, 2021). Again, the term “core” means that a copy of the gene was identified in all seven accessions and “non-core” means that a copy of the gene was identified in less than all seven accessions.

GO-term enrichment analyses were performed in agriGO v2.0 (Tian *et al*., 2017) for core and non-core genes using GO terms available from the Legume Information System (https://www.legumeinfo.org/). The list of all annotated genes identified in the pan-genome (“pan-genes”) that were located on pseudomolecules (Vu01-Vu11) was used as a reference. Given the large number of significantly enriched GO terms on both the core and non-core gene sets, GO slims (Onsongo *et al*., 2008) were extracted and used for the main figure.

Annotation of variants in core and non-core genes

As state above, core and non-core genes are defined based on their frequency of occurrence among the genome assemblies. To test if variants in non-core genes were subject to reduced selective constraint, Variant Effect Predictor (VeP) (McLaren *et al*., 2016) was used to annotate variants identified in core and non-core genes. Gene names from IT97K-499-35 were used to identify genomic intervals that overlap core and non-core genes, and BEDtools intersect (Quinlan & Hall, 2010) was used to filter the VCF file for variants called relative to the IT97K-499-35 assembly using all other assemblies. These VCF files were then annotated in VeP.

A potential issue with comparing core and non-core genes is that noncore genes may be more poorly annotated in some assemblies. To address this, non-core genes that are absent from IT97K-499-35, the most complete assembly, were identified. VeP was run separately for SNPs and indels, reporting classes of variants with potentially large effects, including missense, stop gains, start or stop changes, and frameshifts. As a contrast, the number of synonymous changes and the number of in-frame indels is also reported.

Relative size of core and non-core genes

The physical sizes of core and non-core genes were also compared, both in the total annotated length and the length of the coding portion of each gene. The length of each gene was extracted from the general feature format (GFF) annotation for IT97K-499-35. To estimate the length of coding portion of each gene, the annotated CDS for each gene was extracted from the GFF annotation using scripts built using gffutils (https://github.com/daler/gffutils). The CDS length was calculated based on the primary transcript identified in Phytozome annotations (https://phytozome-next.jgi.doe.gov/cowpeapan/info/Vunguiculata_v1_2). Scripts used in the analysis are available at https://github.com/MorrellLAB/Cowpea_Pangenome.

Nucleotide sequence diversity in cowpea

To determine the level of sequence diversity in the pangenome accessions, we used Tajima's (1983) estimate of $\theta = 4N_e\mu$. We first identified "callable" regions with adequate sequence diversity using coverage estimates in mosdepth (Pederson & Quinlan, 2018), identifying regions with coverage between 5x and 400x in a BED file where coverage across the sequenced accessions in the data was ~200x. This approach is intended to avoid variant calls in regions with inadequate sequence depth or regions where very high coverage may indicate non-unique mapping of sequence reads. The callable regions and the VCF file of filtered variants mapped to the IT97K-499-35 reference were used with pixy (Korunes & Samuk, 2020), a tool designed to deal appropriately with missing data in genome-level resequencing datasets.

Physical locations of SNPs from genotyping platforms

The physical positions of SNPs in the Illumina iSelect Cowpea Consortium Array (Muñoz-Amatriaín *et al*., 2017), whose positions in the IT97K-499-35 genome were provided in Lonardi *et al.* (2019), were mapped using BWA MEM (Li et al., 2009) within each of the seven assemblies using the contextual sequence that flanked each variant. The resulting alignment file was processed with SAMtools (Li *et al*., 2009) and SNP_Utils (https://github.com/MorrellLAB/SNP_Utils) to report positions in a VCF file. The positions of iSelect SNPs relative to all seven genome assemblies are provided in Supplemental Table S02, and an updated summary map for the 51,128 iSelect SNPs in Supplemental Table S03. The positions identified for iSelect SNPs relative to the IT97K-499-35 assembly were used to annotate the variants. The annotation used variant effect predictor (VeP) (McLaren *et al*., 2016) with the GFF file provided by Phytozome (https://genome.jgi.doe.gov/portal/) and SNP positions in VCF files (https://github.com/MorrellLAB/cowpea_annotation/blob/main/Results/IT97K-499-35_v1.0/iSelect_cowpea.vcf; see Data Availability Statement).

Synteny analysis among genome assemblies

In order to assess conservation of gene content and ordering between genome assemblies from diverse species, MCScanX (Wang *et al*., 2012) was run for every genome pair, using default settings and homologous gene pairings derived from gene family assignments defined as the best match of the longest protein product with an E-value of 1e-10 or better from hmmsearch (Eddy 2011) applied to the legfed_v1_0 families (Stai *et al.*, 2019).

Results and Discussion:

Development of six *de novo* assemblies and pan-genome construction

Summary statistics for the seven assemblies (assembly characteristics, repetitive content, genes, BUSCO completeness) are reported in Table 1. More detailed statistics of the intermediate assembly steps are reported in Supplemental Table S04. The contiguity of the new six assemblies, as indicated by their N50s, is comparable to the PacBio assembly for IT97K-499-35 despite being based on short-read sequences. In all six new assemblies, each of the eleven chromosomes of cowpea is represented by a single scaffold. These six assembled genomes are similar in size, ranging from 447.58 Mb to 453.97 Mb, with a mean of 449.91 Mb. IT97K-499-35 had a ~15% larger (more complete) assembled size (519.44 Mb) than these six accessions, with the difference attributable to long-read sequencing and optical mapping providing a more complete assembly. Assemblies of the six additional accessions share the same percentage of

repetitive content of about 45-46% (Table 1 and Supplemental Figure S1). The IT97K-499-35 assembly has a somewhat higher repetitive content, which may result from more completeness of the centromeric regions. The difference between the two sequencing methods is partially attributable to centromeric regions of some chromosomes of the six new accessions appearing to be missing from the assemblies. Centromeric regions were defined based on a 455 bp tandem repeat previously identified by fluorescence in situ hybridization (Iwata Otsubo *et al*., 2016). Supplemental Table S05 shows the coordinates of the putative centromeric regions in IT97K-499-35 for all eleven chromosomes for a total span of 20.18 Mb, in CB5-2 on five chromosomes for a total span of 5.6 Mb, in Sanzi on one chromosome for a total span of 0.59 Mb, in ZN016 on four chromosomes for a total of 7.13 Mb and TZ30 on one chromosome for 1.32 Mb. The tandem repeat was not found in any assembled chromosome of Suvita-2 or UCR779, nor in the other chromosome assemblies where coordinates are not listed.

RNA was prepared from each accession to support gene annotation, and the same annotation protocol was applied to each accession (see Materials & Methods). This is important when comparing genomes at the gene level, as it reduces the technical variability that can otherwise obfuscate the interpretation of results (Lei *et al.* 2021). The number of genes annotated in the six new assemblies ranged from 27,723 to 28,562, with a mean of 28,222 (Table 1). IT97K-499-35 had ~13% more annotated genes with a total of 31,948, reflecting deeper transcriptome sequencing and, to some extent, the more complete assembly of its genome. Supplemental Table S06 summarizes the number of alternative transcripts, exon statistics, gene model support, and ontology annotations (Panther, PFam, KOG, KEGG and E.C.). The number of alternative transcripts in the six new assemblies ranged from 15,088 to 17,115. Again, IT97K-499-35 had a higher number of alternative transcripts, a total of 22,536. The average number of exons was 5.4 in each of the six new assemblies, and 5.2 in IT97K-4899-35, with a median length ranging from 162 to 169 bp. Gene density and repeat density were computed in 1Mb non-overlapping sliding windows along each chromosome and in each accession (Supplemental Figure S1). All chromosomes have a higher gene density in their more recombinationally active regions, while repeat density peaks in the low-recombination centromeric and pericentromeric regions (see also Supplemental Figure 8 in Lonardi *et al*., 2019). All seven accessions have similar gene and repeat density, and high BUSCO v4 completeness at the genome, transcript, and protein levels (Supplemental Table S07), with somewhat higher numbers for IT97K-499-35 than the six new assemblies.

Genes annotated in the seven genomes were classified into *core* if they were present in all accessions and *non-core* if absent in one or more of the seven accessions (see Materials & Methods for details). A total of 21,330 core and 23,531 non-core genes were identified, for a total of 44,861 distinct pan-genome genes (pan-genes) (Supplemental Table 08). From this, it can

be surmised that the number of pan-genes within cultivated cowpeas is more than double the number of genes found in any individual genome.

To determine if adding accessions is likely to significantly change the numbers and proportions of core and non-core genes, the same homology analysis was carried out using subsets of accessions of size *s*=1,2,…,7. For each value of *s*, the number of core and non-core genes was computed for all possible choices of *s* accessions. In Figure 2, the upper curve represents the cumulative number of distinct genes in all accessions (i.e., the set of *pan-genes*), and the lower curve is the number of core genes, as a function of *s* (on the x-axis). Observe that the number of data points for each plotted value of *s* is $\binom{7}{s}$, that is 7 for s=1 or s=6, 21 for s=2 or s=5, 35 for s=3 or s=4. The upper plot is a polynomial fit on the *pan-genes*, while the lower plot is a polynomial fit on the core genes. As expected, the number of pan-genes increased as additional accessions were "added" to the pan-genome, while the number of core genes decreased. However, the fact that the lower plot (core genes) is flattening considerably for s=6 or s=7 indicates that the vast majority of the core genes have been identified with these seven diverse accessions. In contrast, the upper plot is not near flattening, indicating that there may be many more non-core genes not included among these seven accessions, which also means that it would be necessary to sequence more genomes to represent the entire pan-genome of cultivated cowpea thoroughly.

A GO term enrichment analysis was performed for genes within the two components of the pan-genome (core and non-core) using agriGO v2 (Tian *et al*., 2017). Many GO terms for all three ontology aspects (biological process, cellular component, and molecular function) were significantly enriched in both core and non-core genes compared with the entire pan-genome (Supplemental Table S09 for the complete list of significantly enriched terms). Given the high number of significant GO terms, GO Slim terms (Onsongo *et al*., 2008) were extracted and used in Figure 3. Terms highly enriched in the core set of genes were related to protein localization and protein transport, which is part of the broader term 'transport,' and with catabolic processes. This supports the idea that the core genome contains genes that perform essential cellular functions that are highly conserved at the species level. The output was very different for the non-core genes, with very high enrichment of the GO term "stress response" (Figure 3), and in particular with "defense response" ($-\log_{10}q$ = 183.3; Supplemental Table 09). This is consistent with previous research showing that the "dispensable" genome encodes genes involved in defense response and other beneficial functions for some individuals (Golicz *et al*., 2016; Gordon *et al*., 2017; Montenegro *et al*., 2017).

Genetic variation analysis

In addition to identifying gene PAVs (presence/absence variants), the seven assemblies were used to identify other types of variation. Variants were detected using two different software pipelines, depending on their size. SNPs and indels of length up to 300 nucleotides, both considered small variants, were detected using GATK (see Materials & Methods). Larger structural variations, including deletions, duplications, inversions, and translocations, were detected using SyRI (Goel *et al*., 2019).

Across all "callable" regions of the genome, average θ_π = 0.0111 (± 0.0549). At the pseudomolecule-level, average diversity was highest on Vu05, with θ_π = 0.0155 (± 0.0723) and lowest on Vu10 with θ_π = 0.0095 (± 0.0447) (Supplemental Table S10). Mean diversity of ~1% is higher than many grain crops such as barley (Morrell et al. 2014; Schmid et al., 2018) and roughly comparable to maize (Tittes et al., 2021). The observed diversity in the cowpea pangenome sample is above average for herbaceous plants (Miller & Gross, 2011; Leffler et al., 2012; Corbett-Detig et al., 2015).

For SNPs and indels, the genome of each accession was used in turn as the "reference," mapping the reads for each of the six other accessions against that genome. For each, the six SNP sets produced by GATK were merged by taking the union of the SNPs based on their location (i.e., a SNP in two accessions was counted only once if it appeared in the same genomic position). Supplemental Table S11 summarizes the number of SNPs detected, where the reference genome is listed on each row. For instance, using Suvita-2 as the reference, 1,489,850 SNPs were detected using mapped reads from CB5-2, compared to 2,625,678 SNPs using the reads from UCR779. Combining the SNPs by counting all distinct SNPs in the union of the six sets of SNPs, the number of SNPs for Suvita-2 was 5,292,933. When UCR779 was used as the reference, a much higher number of SNPs was detected in every pairwise comparison, indicating that UCR779 is the most divergent among these seven accessions. Conversely, CB5-2 (a California cultivar) has a low number of SNPs with respect to TZ30 and ZN016 (both are from China), relative to other accessions, suggesting that CB5-2 is somewhat more similar to these two accessions than to the other four accessions. This is consistent with genetic assignment analyses reported by Muñoz-Amatriaín *et al.* (2021) and historical considerations discussed in Herniter *et al.* (2020). Supplemental Table S12 provides a similar analysis for indels, where again UCR779 stands out as the most different among the seven accessions. Summary statistics for SNPs and indels for each chromosomes and each accession can be found in the file "SNPs_indels_stats.xlsx" available from the Google Drive indicated in the Data Availability Statement below.

GATK requires a minimum coverage of 5x to call SNPs. Coverage analysis with Mosdepth indicated that the average read coverage of IT97K-499-35 is very high (e.g., about ~190X when

mapping CB5-2 reads to IT97K-4899-35), thus a very high fraction of IT97K-499-35 chromosomes was covered by at least five reads. The lowest was Vu10 with 85.1%, the highest was Vu07 with 98.6%, and the overall percentage of SNPs in IT97K-499-35 that were in a "callable" region (i.e., with coverage 5x-400x) was 88.96%. The frequency SNPs, as the number of unique SNPs identified (Supplemental Table S11) divided by size of the assembled genome (Table 1), ranges from one in 139 to one in 309 bp, and the indel frequency (Supplemental Table S12) ranges from one in 486 to one in 529 bp. Circos plots for SNP density (SNPs per Mb) on each chromosome using each accession as the reference are in Supplemental Figure S2 (A-G), where it is evident, for example, that Vu04 and Vu10 have the highest SNP frequency, while Vu05 and Vu09 have the lowest. This was observed previously when mapping nearly one million SNPs on the IT97K-499-35 reference genome (Lonardi *et al*., 2019). Also, when using UCR779 as the reference (Supplemental Figure S2-E), the number of SNPs on Vu04 and Vu10 is significantly higher than when any other accession is used as the reference, again consistent with UCR779 being the most different among the seven accessions.

Structural variations were identified using SyRI (Goel *et al*., 2019) from the alignment of each pair of individual genomes and visualized using PlotSR (Goel *et al*., 2022) (Figure 4). The visualization shows a relatively large number of structural rearrangements between the seven cowpea genomes, which are more abundant in the centromeric and pericentromeric regions of all chromosomes. Vu04 is the chromosome with the highest abundance of structural variants (Figure 4). A summary statistics of all the structural variants identified in all pairs of accessions is reported in Supplementary Table S13. Observe in the table that Suvita-2 vs UCR779 had the largest number of inversions (2,008) and the largest number of translocations (1,822). This makes sense intuitively since two accessions belong to two different genetic subpopulations that are clearly separated by the first principal component (Figure 1).

SyRI makes use of pairwise alignments to identify syntenic regions among chromosome-level assemblies. For regions that are non-syntenic, SyRI classifies the type of structural variant (i.e., inversion, translocation, duplication) that is most consistent with the pattern of read mapping. This differs from classic structural variant detection approaches, where multiple forms of evidence, such as the distance and orientation of mapped paired-end reads or changes in read coverage are used as evidence of a structural variants. While SyRI is highly dependent on the accuracy of assemblies for both the reference and query sample, the false positive rate for distinguishing syntenic regions from non- syntenic is expected to be low, even if the specific type of structural variant is not classified accurately.

Inversions are a common type of rearrangement with important consequences for cross-over frequency and distribution, as they suppress recombination in heterozygotes (Kirkpatrick, 2010).

While inversion can be important to the maintenance of locally adaptive variants (Kirkpatrick & Barton, 2006), the inhibition of crossover can impede plant breeding efforts. Table 2 summarizes the genomic coordinates of all inversions larger than 1 Mbp. For example, the first column of Table 2 corresponding to IT97K-499-35 shows 27 inversions that were identified by comparing the reference genome against the other six accessions. Observe, however, that the same inversion can appear in multiple sub-tables. For instance, the ~4.2 Mb inversion on chromosome 3 that was previously described in (Lonardi *et al*., 2019) occurs in the same orientation in six accessions and in the opposite orientation only in IT97K-499-35, so it is listed six times in the column for IT97K-499-35. Similarly, the inversion on Vu04 and on Vu05 are detected against five accessions. The ~9.0 Mb inversion on Vu06 is the largest inversion found by SyRI, and its orientation is unique to Suvita-2. However, this inversion appears to be due to an assembly imperfection, as it is reported as unoriented in the ALLMAPS output (Supplemental Table S14) and comparisons between optical maps derived from Suvita-2 and another cowpea accession not included here indicate a non-inverted orientation in Suvita-2 (unpublished). Also, as shown in Lonardi *et al.* (2019) and in Supplemental Figure S3, this entire region has a very low recombination rate, and it comprises nearly the entire short arm of acrocentric chromosome 6 (Iwata-Otsubo *et al*., 2016). These factors can account for a spurious orientation assignment for this region in the Suvita-2 Vu06 assembly.

The positions of the largest inversions shown in Figure 4 are provided in Table 2, e.g., the inversions on Vu03 in IT97K-499-35 reported by Lonardi *et al*. (2019), and the inversion on Vu06 in Suvita-2 likely due to a mis-assembly, as discussed above. It should be noted that regions with apparently low synteny within of several chromosomes are low-recombination centromeric and pericentromeric regions (Lonardi *et al*., 2019), which are notoriously hard to assemble due to their high repetitive content, and hard to orient due to a paucity of mapped and recombinationally ordered SNPs. In these regions, it is expected to have compressed contigs, gaps and mis-assemblies, any of which might be flagged as apparent structural variations. The number of such false-positive structural variations can likely be reduced by increasing the completeness of the assemblies within these regions using long-read sequencing and optical mapping. Supplemental Figures 4A-4U show all 21 SyRi+PlotSR alignments between all pairs of cowpea accessions in this study.

Further characterization of core and non-core genes

Partitioning SNPs into those found in core versus noncore genes resulted in 481,655 SNPs in core genes and 461,522 SNPs in noncore genes. The indel comparison involves 120,686 indels in core genes and 80,182 noncore genes. Core and noncore genes have similar numbers of potentially benign mutations, including synonymous and in-frame indels. Mutations that VeP

classifies as more likely to be harmful, including missense changes, stop gains, and frameshift mutations are much more abundant in noncore genes (Figure 5). These variants are summarized in Supplemental Table S15. Counting both SNPs and indels, among core genes there are 93,559 potentially benign (synonymous and in-frame indel) variants relative to 86,802 potentially harmful variants, a ratio of 1.08. For noncore genes, this ratio was 108,277/196,667 = 0.55 (Supplemental Table S15). Noncore genes are notable for having a particularly large number of frameshift variants (Figure 5).

Based on the gene annotations in the GFF files, core genes were longer than noncore genes, with a difference in mean length of 4,257.91 (± 3920.48) versus 3,010.59 bp (± 3971.48) (with median lengths of 3,367 and 1,850), respectively. This difference is significant based on a non-parametric, two-sample Wilcoxon rank sum test, with p-value < 2.2e-16. Relative to annotations in IT97K-499-35, this means that core genes cover 90.8 Mb of the genome while noncore genes cover 32.0 Mb. Differences in total gene length for individual core and noncore genes could result from either longer coding regions or longer or more abundant introns. After extracting the coding sequence (CDS) for each gene, we also found that the mean length of the coding portion of core genes is longer than noncore genes with a mean of 1,294.96 (± 924.74) versus 1,085.68 bp (± 1,032.00). Based on the Wilcoxon test the difference in length of the coding sequence is significant with a p-value < 2.2e-16.

Presence/absence variation of genes controlling black seed coat color

In order to facilitate use of the cowpea pan-genome by the community, all the genomes and their annotations have been included as resources in the Legume Information System (LIS; www.legumeinfo.org; Dash *et al*., 2016). As an example of a use case for pan-genomics within the context of that system, the Genome Context Viewer (GCV) is an application that enables dynamic comparison of genomes based on their gene content, using assignments of genes to families as the basis for computation and visualization of conserved gene order and structural variation with potential impact on function, e.g. copy number variation (CNV) and presence/absence variation (PAV) (Cleary and Farmer, 2018) Figure 6A shows the results of a query centered on a region from the reference cowpea genome that features a cluster of tandemly duplicated MYB transcription factor genes in which presence/absence variation was previously determined to be associated with seed coat pigmentation (Herniter et al., 2018). Colors of the genes in this “beads on a string” representation reflect the gene family assignments; here, the brown triangles in the center of the region represent the MYB genes with varying copy numbers in the different cowpea accessions, with a maximum of five copies in the reference accession to as few as a single copy in UCR779. Outside the CNV region, there is strong conservation of gene content, with one other region showing some evidence of reordering among the cowpea

accessions. The viewer facilitates comparison not only within but across species, and one can see evidence of similar CNV in the corresponding region of several *Phaseolus* spp. genomes (Schmutz *et al*. 2014, Moghaddam *et al.* 2021), as well as an inversion of the segment containing the genes relative to cowpea, soybean (Valliyodan *et al.* 2019) and other *Vigna* species (Sakai *et al*. 2015, Kang *et al.* 2014). The most recent whole genome duplication in soybean is evidenced by two corresponding homoeologous regions; interestingly, the region serves as a breakpoint for the syntenic block in Gm09, which taken together with the other structural variation suggests that the expansion of gene copy number here has had consequences for the stability of the chromosome in these regions over evolutionary time (Hastings et al., 2009).

Although the GCV view shows good evidence for CNV, there are some limitations to what may be inferred from that alone. First, since the viewer only has access to gene family assignment information, it is unable to determine which elements among those in tandem arrays actually have the highest sequence similarity and provide insight into which copies have been deleted. Second, because it relies on the surrounding genomic context of each gene to place it into correspondence, it will have limited capability for finding genes that are present in the assembly but are largely isolated on small scaffolds that were not incorporated into the main pseudomolecules. Another tool at LIS that provides a complementary view based on the underlying sequence identity of the different copies of the expanded gene family is shown in Figure 6B. Here, the InterMine (Kalderamis *et al*., 2014) instance for cowpea (https://mines.legumeinfo.org/cowpeamine/begin.do) was used to collect all protein sequences for cowpea genes assigned to the given family and a dynamic tree construction procedure invoked based on hmmalign-derived (http://www.csb.yale.edu/userguides/seq/hmmer/docs/node18.htmlxxxEddy, 2011) additions of these genes to the multiple sequence alignment for the founding members of the family. The resulting tree (a subtree of which is shown) allows the user to determine the best correspondences of the copies in each genome and also pulls in a couple of genes on unanchored contigs that likely belong to the region.

Pangenome core genes and cross-species synteny

To explore the question of how within-species gene content conservation compares with gene content shared between species in other species and genera, we used the LIS gene family assignments to define homology pairings for between all members of each gene family, then used the resulting data to define collinearity blocks among all pairwise comparisons of the cowpea genomes, as well as to soybean and representative genomes from *Vigna* and *Phaseolus* spp. The counts of genes participating in at least one collinear block were tallied for each genome in each pairwise comparison. As expected, intra-specific comparisons between cowpea accessions yield higher numbers of conserved collinear genes than inter-specific comparisons.

On the other hand, there is no appreciable difference in the extent of conserved collinearity when comparing cowpea genomes to other species within the *Vigna* genus versus species from *Phaseolus* or *Glycine* genera (Supplemental Figure S05). Because soybean has an additional whole genome duplication relative to all other species in the comparison, the total number of soybean genes found in collinear blocks in that comparison is higher than in other comparisons. Comparisons between all species and the *Vigna radiata* version 6 genome (Kang *et al*. 2014) show fewer conserved collinear genes, but this is presumably due to missing data in that assembly given that all other interspecific comparisons are similar.

Data Availability Statement. The genome assemblies and annotations described in this manuscript all are available from CowpeaPan (https://phytozome-next.jgi.doe.gov/cowpeapan). Raw DNA and RNA sequence data from IT97K-499-35, and whole genome shotgun DNA sequences for 36 diverse cowpea accessions used for SNP discovery in Muñoz-Amatriaín *et al.* (2017) are available from NCBI as stated in Lonardi *et al*. (2019). Raw DNA and RNA sequence data from the six additional accessions providing de novo assemblies in this report, and sequences produced by 10X Genomics from IT97K-49-35, are available as BioProject PRJNA836573 from the National Center for Biotechnology Information (NCBI). More complete annotation files, assemblies and SNPs are also available from the shared Google drive link https://drive.google.com/drive/folders/1iQaLW4SLmN2lP7q4k3uovHK3SvsxGbVi?usp=sharing .

Acknowledgments. The authors thank Staff Research Associate Yi-Ning Guo (UCR) for RNA preparation; Programmer Steve Wanamaker (UCR) for informatics assistance; Jeffrey Ehlers (Bill & Melinda Gates Foundation), Phillip Roberts (UCR) and Anthony Hall (UCR) for discussions on the accessions for sequencing; Bao Lam Huynh (UCR) and Mitchell Lucas (UCR) for assistance with greenhouse operations for pure seed production; Richard Hayes (Department of Energy Joint Genome Institute) for assistance with Phytozome; and Samuel Hokin (National Center for Genome Resources) for data curation for loading data into CowpeaMine. Hardware and software support were also provided by the University of Minnesota Supercomputing Institute.

Conflict of Interest. The authors declare no conflict of interest.

Funder Information. Development of an initial pan-genome of domesticated cowpea (*Vigna unguiculata* ssp. *unguiculata* [L.] Walp.) was an objective of the National Science Foundation BREAD project "Advancing the Cowpea Genome for Food Security" (IOS 1543963). Funding was also provided by NSF IIS-1814359 ("Improving de novo Genome Assembly using Optical Maps"). The work conducted by the US Department of Energy Joint Genome Institute, a DOE Office of Science User Facility, was supported by the Office of Science of the US Department of Energy under Contract No. DE-AC02-05CH11231. Support for the work of ADF provided by the U.S. Department of Agriculture, Agricultural Research Service, Non-Assistance Cooperative Agreement 58-5030-7-069. This work also benefited from and addressed breeding and germplasm management objectives of the Feed the Future Innovation Lab for Climate Resilient Cowpea (USAID Cooperative Agreement AID-OAA-A-13-00070). Partial support was also provided by the National Natural Science Foundation of China (32172568), the Major Science and Technology Project of Plant Breeding in Zhejiang Province (2021C02065-6-3) and the

National Ten-Thousand Talents Program of China (to PX). Partial support was also provided by Hatch Project CA-R-BPS-5306-H.

Literature Cited

Aggarwal VD, Muleba N, Drabo I, Souma J, Mbewe M (1984) Inheritance of *Striga gesnerioides* resistance in cowpea. In: Proceedings of 3rd International Symposium on Parasitic Weeds (Parker C, Musselman LJ, Polhill RM, Wilson AK eds.) ICARDA, Aleppo, Syria, pp. 143-147

Bayer PE, Golicz AA, Scheben A, Batley J, Edwards D (2020) Plant pan-genomes are the new reference. Nature Plants 6:914-920.

Boukar O, Belko N, Chamarthi S, Togola A, Batieno J, Owusu E, Haruna M, Diallo S, Umar ML, Olufajo O, Fatokun C (2019) Cowpea (*Vigna unguiculata*): Genetics, genomics and breeding. Plant Breeding 138:415-424, doi.org/10.1111/pbr.12589

Boukar O, Bhattacharjee R, Fatokun C, Kumar PL, Gueye B (2013) Cowpea. In: Genetic and Genomic Resources of Grain Legume Improvement (Singh M, Upadhyaya HD, Bisht IS eds.), Chapter 6, pp. 137-156, Elsevier, London, UK. ISBN 978-0-12-397935-3

Cao J, Schneeberger K, Ossowski S, Günther T, Bender S, Fitz, J, Koenig D, Lanz C, Stegle O, Lippert C, Wang X, Ott F, Müller J, Alonso-Blanco C, Borgwardt K, Schmid KJ, Weigel D (2011) Whole-genome sequencing of multiple *Arabidopsis thaliana* populations. Nature Genetics 43:956–963, doi.org/10.1038/ng.911

Chapman JA, Ho I, Sunkara S, Luo S, Schroth GP, Rokhsar DS (2011) Meraculous: *de novo* genome assembly with short paired-end reads. PLOS ONE 6:e23501

Cleary A, Farmer A (2018) Genome Context Viewer: visual exploration of multiple annotated genomes using microsynteny. Bioinformatics34:1562-1564, doi: 10.1093/bioinformatics/btx757

Corbett-Detig RB, Hartl DL, Sackton TB (2015) Natural selection constrains neutral diversity across a wide range of species. PLOS Biology 13:e1002112, doi: 10.1371/journal.pbio.1002112

Darling AE, Mau B, Perna NT (2010) progressiveMauve: multiple genome alignment with gene gain, loss and rearrangement. PLOS ONE 5:e11147, doi.org/10.1371/journal.pone.0011147

Dash S, Campbell JD, Cannon EK, Cleary AM, Huang W, Kalberer SR, Karingula V, Rice AG, Singh J, Umale PE, Weeks NT, Wilkey AP, Farmer AD, Cannon SB. (2016) Legume

information system (LegumeInfo.org): a key component of a set of federated data resources for the legume family. Nucleic Acids Research 44:D1181-1188, doi: 10.1093/nar/gkv1159

de Mooy BE (1985) Germplasm evaluation of Botswana cowpea (*Vigna unguiculata* [L.] Walp.) landraces. M.S. Thesis, Michigan State University, Lansing, Michigan, USA.

Eddy SR. (2011) Accelerated Profile HMM Searches. PLoS Computational Biology 7:e1002195, doi: 10.1371/journal.pcbi.1002195.

Ehlers JD, Fery RL, Hall AE (2002) Cowpea breeding in the USA: new varieties and improved germplasm. *In* Challenges and Opportunities for Enhancing Sustainable Cowpea Production. Proceedings of the World Cowpea Conference III held at the International Institute of Tropical Agriculture (IITA), Ibadan, Nigeria, 4-8 September 2000, (Eds. Fatokun CS, Tarawali SA, Singh BB, Kormawa PM, Tamò M), Chapter 1.6, pp. 62-77, IITA, Ibadan, Nigeria, ISBN 978-131-190-8

Goel M, Schneeberger K (2022) plotsr: visualizing structural similarities and rearrangements between multiple genomes. Bioinformatics 38:2922-2926, doi.org/10.1093/bioinformatics/btac196

Goel M, Sun H, Jiao W-B, Schneeberger K (2019) SyRI: finding genomic rearrangements and local sequence differences from whole-genome assemblies. Genome Biology 20:277, doi:10.1186/s13059-019-1911-0

Golicz AA, Bayer PE, Bhalla PL, Batley J, Edwards D (2020) Pangenomics comes of age: from bacteria to plant and animal applications. Trends in Genetics 36:132-145

Golicz AA, Bayer PE, Barker GC, Edger PP, Kim HR, Martinez PA, Chan CKK, Severn-Ellis A, McCombie R, Parkin IAP, Paterson AH, Pires JC, Sharpe AG, Tang H, Teakle GR, Town CD, Bately J, Edwards D (2016) The pangenome of an agronomically important crop plant *Brassica oleracea*. Nature Communications 7:13390, doi.org/10.1038/ncomms13390

Gordon SP, Contreras-Moreira B, Woods DP, Des Marais DL, Burgess D, Shu S, Stritt C, Roulin AC, Schackwitz W, Tyler L, Martin J, Lipzen A, Dochy N, Phillips J, Barry K, Geuten K, Budak H, Juenger TE, Amasino R, Caicedo AL, Goodstein D, Davidson P, Mur LAJ, Figueroa M, Freeling M, Catalan P, Vogel JP (2017) Extensive gene content variation in the *Brachypodium distachyon* pan-genome correlates with population structure. Nature Communications 8:2184, doi.org/10.1038/s41467-017-02292-8

Haas BJ, Delcher AL, Mount SM, Wortman JR, Smith Jr RK, Hannick LI, Maiti R, Ronning CM, Rusch DB, Town CD, Salzberg SL, White O (2003) Improving the *Arabidopsis* genome annotation using maximal transcript alignment assemblies. Nucleic Acids Research 31:5654-5666, http://nar.oupjournals.org/cgi/content/full/31/19/5654

Hastings PJ, Lupski JR, Rosenberg SM, Ira G (2009) Mechanisms of change in gene copy number. Nature Review Genetics 10:551-564, doi: 10.1038/nrg2593. PMID: 19597530; PMCID: PMC2864001.

Hall AE (2004) Breeding for adaptation to drought and heat in cowpea. European Journal of Agronomy 21:447-454

Herniter IA, Muñoz-Amatriaín M, Close TJ (2020) Genetic, textual, and archeological evidence of the historical global spread of cowpea (*Vigna unguiculata* [L.] Walp.). Legume Science 3:57

Herniter IA, Muñoz-Amatriaín M, Lo S, Guo Y-N, Close TJ (2018) Identification of candidate genes controlling black seed coat and pod tip color in G3 8:3347-3355

Hirsch CN, Foerster JM, Johnson JM, Sekhon RS, Muttoni G, Vaillancourt B, Peñagaricano F, Lindquist E, Pedraza MA, Barry K, de Leon N, Kaeppler SM, Buell CR (2014) Insights into the maize pan-genome and pan-transcriptome. The Plant Cell 26:121–135

Iwata-Otsubo A, Lin J-Y, Gill N, Jackson SA (2016) Highly distinct chromosome structures in cowpea (*Vigna unguiculata*), as revealed by molecular cytogenetic analysis. Chromosome Research 24:197-216

Kalderimis A, Lyne R, Butano D, Contrino S, Lyne M, Heimbach J, Hu F, Smith R, Stěpán R, Sullivan J, Micklem G (2014) InterMine: extensive web services for modern biology. Nucleic Acids Research 42:W468-472, doi: 10.1093/nar/gku301

Kang YJ, Kim SK, Kim MY, Lestari P, Kim KH, Ha BK, Jun TH, Hwang WJ, Lee T, Lee J, Shim S, Yoon MY, Jang YE, Han KS, Taeprayoon P, Yoon N, Somta P, Tanya P, Kim KS, Gwag JG, Moon JK, Lee YH, Park BS, Bombarely A, Doyle JJ, Jackson SA, Schafleitner R, Srinives P, Varshney RK, Lee SH (2014) Genome sequence of mungbean and insights into evolution within *Vigna* species. Nature Communications 5:5443, doi: 10.1038/ncomms6443

Kent WJ (2002) BLAT - the BLAST-like alignment tool. Genome Research 12:656-64

Kirkpatrick M (2010) How and why chromosome inversions evolve. PLOS Biology 8:e1000501

Kirkpatrick M, Barton N (2006) Chromosome inversions, local adaptation and speciation. Genetics 173:419-434

Korunes KL, Samuk K (2021) PIXY: Unbiased estimation of nucleotide diversity and divergence in the presence of missing data. Molecular Ecology Resources 21:1359-1368

Leffler EM, Bullaughey K, Matute DR, Meyer WK, Ségurel L, Venkat A, Andolfatto P, Przeworski M (2012) Revisiting an old riddle: what determines genetic diversity levels within species. PLOS Biology 10:e1001388

Lei L, Goltsman E, Goodstein D, Wu GA, Rokhsar DS, Vogel JP (2021) Plant pan-genomics comes of age. Annual Reviews of Plant Biology 72:411-435

Li H (2018) Minimap2: pairwise alignment for nucleotide sequences. Bioinformatics 34:3094-3100

Li H, Durbin R (2009) Fast and accurate short read alignment with Burrows–Wheeler transform. Bioinformatics 25:1754–1760

Li H, Handsaker B, Wysoker A, Fennell T, Ruan J, Homer N, Marth G, Abecasis G, Durbin R (2009) 1000 Genome Project Data Processing Subgroup, The Sequence Alignment/Map format and SAMtools. Bioinformatics 25:2078–2079

Li YH, Zhou G, Ma J, Jiang W, Jin LG, Zhang Z, Guo Y, Zhang J, Sui Y, Zheng L, Zhang SS, Zuo Q, Shi XH, Li YF, Zhang WK, Hu Y, Kong G, Hong HL, Tan B, Song J, Liu ZX, Wang Y, Ruan H, Yeung CKL, Liu J, Wang H, Zhang LJ, Guan RX, Wang KJ, Li WB, Chen SY, Chang RZ, Jiang Z, Jackson SA, Li R, Qiu LJ (2014) *De novo* assembly of soybean wild relatives for pan-genome analysis of diversity and agronomic traits. Nature Biotechnology 32:1045–1052, doi.org/10.1038/nbt.2979

Liang Q, Lonardi S (2021) Reference-agnostic representation and visualization of pan-genomes. BMC Bioinformatics 22:502

Lonardi S, Muñoz-Amatriaín M, Liang Q, Shu S, Wanamaker SI, Lo S, Tanskanen J, Schulman AH, Zhu T, Luo MC, Alhakami H, Ounit R, Hasan AM, Verdier J, Roberts PA, Santos JRP, Ndeve A, Doležel J, Vrána J, Hokin SA, Farmer AD, Cannon SB, Close TJ (2019) The genome of cowpea (*Vigna unguiculata* [L.] Walp.). The Plant Journal 98:767-782

Mackie WW (1946) Blackeye beans in California. Bulletin 696, University of California Agricultural Experiment Station

McLaren W, Gil L, Hunt SE, Riat HS, Ritchie GRS, Thormann A, Flicek P, Cunningham F (2016) The Ensembl variant effect predictor. Genome Biology 17:122

Miller AJ, Gross BL (2011) From forest to field: perennial fruit crop domestication. American Journal of Botany 98:1389-1414

Moghaddam SM, Oladzad A, Koh C, Ramsay L, Hart JP, Mamidi S, Hoopes G, Sreedasyam A, Wiersma A, Zhao D, Grimwood J, Hamilton JP, Jenkins J, Vaillancourt B, Wood JC, Schmutz J, Kagale S, Porch T, Bett KE, Buell CR, McClean PE (2021) The tepary bean genome provides insight into evolution and domestication under heat stress. Nature Communications 12:2638, doi: 10.1038/s41467-021-22858-x

Montenegro JD, Golicz AA, Bayer PE, Hurgobin B, Lee H, Chan C-KK., Visendi P, Lai K, Doležel J, Batley J, Edwards D (2017) The pangenome of hexaploid bread wheat. The Plant Journal 90:1007-1013, doi.org/10.1111/tpj.13515

Morgante M, De Paoli E, Radovic S (2007) Transposable elements and the plant pan-genomes. Current Opinions in Plant Biology 10:149–155

Morrell PL, Gonzales AM, Meyer KKT, Clegg MT (2014) Resequencing data indicate a modest effect of domestication on diversity in barley: a cultigen with multiple origins. Journal of Heredity 105:253-264, doi: 10.1093/jhered/est083

Muñoz-Amatriaín M, Eichten SR, Wicker T, Richmond TA, Mascher M, Steuernagel B, Scholz U, Ariyadasa R, Spannagl M, Nussbaumer T, Mayer KF, Taudien S, Platzer M, Jeddeloh JA, Springer NM, Muehlbauer GJ, Stein N (2013) Distribution, functional impact, and origin mechanisms of copy number variation in the barley genome. Genome Biology 14:R58

Muñoz-Amatriaín M, Lo S, Herniter IA, Boukar O, Fatokun C, Carvalho M, Castro I, Guo Y-N, Huynh B-L, Roberts PA, Carnide V, Close TJ (2021) The UCR Minicore: a resource for cowpea research and breeding. Legume Science 3:e95, doi.org/10.1002/leg3

Muñoz-Amatriaín M, Mirebrahim H, Xu P, Wanamaker SI, Luo M, Alhakami H, Alpert M, Atokple I, Batieno BJ, Boukar O, Bozdag S, Cissé N, Drabo I, Ehlers JD, Farmer A, Fatokun C, Gu YQ, Guo Y, Huynh B, Jackson SA, Kusi F, Lawley CT, Lucas MR, Ma Y, Timko MP,

Wu J, You F, Barkley NA, Roberts PA, Lonardi S, Close TJ (2017) Genome resources for climate-resilient cowpea, an essential crop for food security. The Plant Journal 89:1042-1054

Onsongo G, Xie H, Griffin TJ, Carlis (2008) Generating GO slim using relational database management systems to support proteomics analysis. 21st IEEE International Symposium on Computer-Based Medical Systems, doi.org/10.1109/CBMS.2008.77

Pedersen BS, Quinlan AR (2018) Mosdepth: quick coverage calculation for genomes and exomes. Bioinformatics 34:867–868, doi.org/10.1093/bioinformatics/btx699

Quinlan AR, Hall IM (2010) BEDtools: a flexible suite of utilities for comparing genomic features. Bioinformatics 26:841-841

Sakai H, Naito K, Ogiso-Tanaka E, Takahashi Y, Iseki K, Muto C, Satou K, Teruya K, Shiroma A, Shimoji M, Hirano T, Itoh T, Kaga A, Tomooka N (2015) The power of single molecule real-time sequencing technology in the de novo assembly of a eukaryotic genome. Scientific Reports 5:16780, doi: 10.1038/srep16780.

Salamov AA, Solovyev VV (2000) *Ab initio* gene finding in *Drosophila* genomic DNA. Genome Research 10:516-522

Schmid K, Kilian B, Russell J (2018) Barley Domestication, Adaptation and Population Genomics. editors. In: Stein N, Muehlbauer G (eds.) The Barley Genome. Compendium of Plant Genomes. Springer, Cham. pp. 317-336.

Schmutz J, McClean PE, Mamidi S, Wu GA, Cannon SB, Grimwood J, Jenkins J, Shu S, Song Q, Chavarro C, Torres-Torres M, Geffroy V, Moghaddam SM, Gao D, Abernathy B, Barry K, Blair M, Brick MA, Chovatia M, Gepts P, Goodstein DM, Gonzales M, Hellsten U, Hyten DL, Jia G, Kelly JD, Kudrna D, Lee R, Richard MM, Miklas PN, Osorno JM, Rodrigues J, Thareau V, Urrea CA, Wang M, Yu Y, Zhang M, Wing RA, Cregan PB, Rokhsar DS, Jackson SA (2014) A reference genome for common bean and genome-wide analysis of dual domestications. Nature Genetics 46:707-713, doi: 10.1038/ng.3008

Shu S, Goodstein D, Rokhsar D (2013) PERTRAN: genome-guided RNA-seq read assembler. https://www.osti.gov/biblio/1241180

Shu S, Rokhsar D, Goodstein D, Hayes D, Mitros T (2014) JGI plant genomics gene annotation pipeline. Lawrence Berkeley National Laboratory, Berkeley, CA, USA

Singh BB, Olufajo OO, Ishiyaku MF, Adeleke RA, Ajeigbe HA, Mohammed SG (2006) Registration of six improved germplasm lines of cowpea with combined resistance to *Striga gesnerioides* and *Alectra vogelii*. Crop Science 46:2332-2333

Springer NM, Ying K, Fu Y, Ji T, Yeh CT, Jia Y, Wu W, Richmond T, Kitzman J, Rosenbaum H, Iniguez AL, Barbazuk WB, Jeddeloh JA, Nettleton D, Schnable PS (2009) Maize inbreds exhibit high levels of copy number variation (CNV) and presence/absence variation (PAV) in genome content. PLoS Genetics 5:e1000734

Stai JS, Yadav A, Sinou C, Bruneau A, Doyle JJ, Fernández-Baca D, Cannon SB (2019) Cercis: a non-polyploid genomic relic within the generally polyploid legume family. Frontiers in Plant Science 10:345, doi: 10.3389/fpls.2019.00345

Tajima F (1983) Evolutionary relationship of DNA sequences in finite populations. Genetics 105:437-460

Tang H, Zhang X, Miao C, Zhang J, Ming R, Schnable JC, Schnable PS, Lyons E, Lu J (2015) ALLMAPS: robust scaffold ordering based on multiple maps. Genome Biology 16:3, doi:10.1186/s13059-014-0573-1

Tian T, Liu Y, Yan H, You Q, Yi X, Du Z, Xu W, Su Z (2017) agriGO v2.0: a GO analysis toolkit for the agricultural community, 2017 update. Nucleic Acids Research 45:W122-W129, doi: 10.1093/nar/gkx382

Tittes S, Lorant A, McGinty S, Doebley JF, Holland JB, de Jesus Sánchez-González, Seetharam A, Tenaillon M, Ross-Ibarra J (2021) Not so local: the population genetics of convergent adaptation in maize and teosinte. bioRxiv, doi: 10.1101/2021.09.09.459637

Torkamaneh D, Lemay M-A, Belzile F (2021) The pan-genome of the cultivated soybean (PanSoy) reveals an extraordinarily conserved gene content. Plant Biotechnology Journal 19:1852-1862, https://doi.org/10.1111/pbi.13600

Valliyodan B, Cannon SB, Bayer PE, Shu S, Brown AV, Ren L, Jenkins J, Chung CY, Chan TF, Daum CG, Plott C, Hastie A, Baruch K, Barry KW, Huang W, Patil G, Varshney RK, Hu H, Batley J, Yuan Y, Song Q, Stupar RM, Goodstein DM, Stacey G, Lam HM, Jackson SA, Schmutz J, Grimwood J, Edwards D, Nguyen HT (2019) Construction and comparison of three reference-quality genome assemblies for soybean. The Plant Journal 100:1066-1082, doi: 10.1111/tpj.14500

Wang Y, Tang H, Debarry JD, Tan X, Li J, Wang X, Lee TH, Jin H, Marler B, Guo H, Kissinger JC, Paterson AH (2012) MCScanX: a toolkit for detection and evolutionary analysis of gene synteny and collinearity. Nucleic Acids Research 40:e49, doi: 10.1093/nar/gkr1293

Xu P, Wu X, Muñoz-Amatriaín M, Wang B, Wu X, Hu Y, Huynh BL, Close TJ, Roberts PA, Zhou W, Lu Z, Li G (2017) Genomic regions, cellular components and gene regulatory basis underlying pod length variations in cowpea (*V. unguiculata* L. Walp). Plant Biotechnology Journal 15:547-557, doi:10.1111/pbi.12639

Yeh R-F, Lim LP, Burge CB (2001) Computational inference of homologous gene structures in the human genome. Genome Research 11:803-816

Yu G, Wang L, Han Y, He Q (2012). clusterProfiler: an R package for comparing biological themes among gene clusters. OMICS: A Journal of Integrative Biology 16:284-287, doi:10.1089/omi.2011.0118

Title: A view of the pan-genome of domesticated cowpea (*Vigna unguiculata* [L.] Walp.)

Figure and Table Captions

Figure 1. Principal component analysis of the UCR Minicore, indicating the accessions selected for sequencing and the subpopulation they belong to. Accessions in the plot are colored by the result of STRUCTURE for *K=6*, as shown in Muñoz- Amatriaín *et al.* (2021).

Figure 2. The number of genes identified in the pan-genome (pan-genes) and core genome (core genes) as new accessions are added. The red curve represents the cumulative number of distinct genes in all accessions (i.e., the set of *pan-genes*), while the blue curve represents the number of core genes (dispensable plus private), as a function of the number of accessions considered in the range 1-7. The shaded area represents the spread on the number of genes for each choices of number of accessions.

Figure 3. Gene Ontology (GO) term enrichment analysis. Significantly enriched GO terms for core (A) and noncore genes (B) are shown for GO-Slim categories belonging to Biological Process, Cellular Component, and Molecular Function aspects (in different colors). -log10 of FDR-adjusted p-values (q-values) are shown on the right of each bar.

Figure 4. Representation of structural variations (of any size) detected by SyRI from the output of whole-genome pairwise alignments between the seven cowpea accessions. The black track indicates gene density in the reference genome IT97K-499-35, while the blue track indicates SNP density in the reference genome IT97K-499-35.

Figure 5. Variant effect predictor (VeP) annotations for SNPs and indels found in the core and noncore genes present in IT97K-499-35. Values on the y-axis are the absolute number of variants in each variant class.

Figure 6. Conservation of gene content within and across species. (A) A region depicting gene content conservation and variability among cowpea genomes and other representative Phaseoleae species. Triangular glyphs represent order and orientation of genes, with color representing gene family memberships. (https://vigna.legumeinfo.org/tools/gcv) (B) All cowpea proteins assigned to the family whose members exhibit copy number variation in (A) are shown augmenting a dynamically recomputed gene tree at the Legume Information System, with genes from unanchored contigs not present in the chromosomes aligned in (A) indicated with arrows (https://mines.legumeinfo.org/cowpeamine).

Table 1. Summary of assembly statistics, repetitive content, gene content and BUSCO completeness.

Table 2. Genomic coordinates of all inversions of size > 1 Mbp detected by comparing the seven cowpea genomes pairwise (IT97K- 499-35 is abbreviated as IT97K).

Supplemental Figure S1. Gene and repeat density. Accessions are represented by different shades of red (genes) and blue (repeats). The reference genome of IT97K-499-35 is the longest curve, i.e., the one that extends furthest to the right of each graph.

Supplemental Figure S2. SNP density (number of SNPs per Mb) using each individual genome as the "reference". (A) IT97K-499-35 (IT97K), centromeres are marked with orange in the innermost circle, (B) CB5-2, (C) Suvita-2, (D) Sanzi, (E) UCR779, (F) ZN016, (G) TZ30.

Supplemental Figure S3. Output of ALLMAPS for chromosome Vu06 for Suvita-2. Ten genetic maps were used to orient the five Dovetail contigs in Vu06 (two of which larger than 1Mb – see Supplemental Table S14). The first four were arbitrarily oriented by ALLMAPS due to low recombination in that region, as shown on the graphs on the right, which plot cM position (y-axis) as a function of physical position (x-axis). In particular, the 8.2Mb contig represented in gray in the bottom left figure, is a region of very low recombination frequency and was likely oriented incorrectly.

Supplemental Figure S4. Structural variants (of any size) detected by SyRI between any pairs of genomes in this study. (A) CB5-2 vs Sanzi, (B) CB5-2 vs Suvita-2, (C) CB5-2 vs TZ30, (D) CB5-2 vs UCR779, (E) CB5-2 vs ZN016, (F) IT97K-499-35 vs CB5-2, (G) IT97K-499-35 vs Sanzi, (H) IT97K-499-35 vs Suvita-2, (I) IT97K-499-35 vs TZ30, (J) IT97K-499-35 vs UCR779, (K) IT97K-499-35 vs ZN016, (L) Sanzi vs TZ30, (M) Sanzi vs UCR779, (N) Sanzi vs ZN016, (O) Suvita-2 vs Sanzi, (P) Suvita-2 vs TZ30, (Q) Suvita-2 vs UCR779, (R) Suvita-2 vs ZN016, (S) UCR779 vs TZ30, (T) UCR779 vs ZN016, (U) ZN016 vs TZ30.

Supplemental Figure S5. **Macrosynteny views.** (A) Macrosynteny view with blocks representing regions in the IT97K-499-35 reference cowpea genome with conserved gene order relative to each of the genomes shown as tracks below. The region from the microsynteny view of Figure 6A is shown with a vertical gray bar, and the set of chromosomes displayed is restricted to those showing synteny in that region (i.e. the non-cowpea chromosomes have an apparent lack of synteny downstream because of genomic rearrangements that have moved corresponding content to other chromosomes than those shown). Various inversions are seen as blocks with orientations opposing those of their neighboring blocks, and gaps in otherwise syntenic regions indicate regions in which gene content diversity outweighs conserved content through presence-absence and copy-number variation. (B) Counts of genes participating in conserved collinear blocks for all pairwise genome comparisons among the cowpea pangenome

members and across representative genomes from several genera in the Phaseoleae tribe. Self-comparisons are included to illustrate within-species conservation of duplicated content from ancient whole genome duplication (WGD) event shared by subfamily Faboideae species, as well as the more recent WGD in the *Glycine max* genome.

Supplemental Table S01. Cowpea accessions used in this work.

Supplemental Table S02. Cowpea iSelect SNP positions on each of the seven genome assemblies.

Supplemental Table S03. Cowpea iSelect arrray SNP positions and alleles relative to the IT97K-499-35 sequence of Lonardi et al. 2019 and the iSelect "Forward Strand".

Supplemental Table S04. Statistics of the six new assemblies at each step of the Dovetail assembly pipeline.

Supplemental Table S05. Putative centromeric region coordinates (all numbers are bp).

Supplemental Table S06. Gene annotation statistics.

Supplemental Table S07. BUSCO v4 completeness results.

Supplemental Table S08. List of core and non-core genes identified from sequencing the seven cowpea genomes.

Supplemental Table S09. Enrichment analysis of GO Terms for core genes and noncore genes performed in AgriGO v2.

Supplemental Table S10. Average diversity at the chromosome (pseudomolecule) level relative to the IT97K-4899-35 assembly. Values reported are $\theta\pi$ and the standard deviation for “callable regions.”

Supplemental Table S11. Number of SNPs when considering each accession as the “reference” genome, and the resulting union of unique SNPs (merged GVCF) for each accession.

Supplemental Table S12. Number of indels of size 1 to 300 bp when considering each accession as the “reference” genome, and the union set of all indels (merged GVCF) for each accession.

Title: A view of the pan-genome of domesticated cowpea (*Vigna unguiculata* [L.] Walp.)

Supplemental Table S13. Genomic coordinates of all structural variants detected via SyRI by comparing the seven cowpea genomes pairwise. IT97K-499-35 is abbreviated as IT97K.

Supplemental Table S14. Largest inversions, using each of the Dovetail assemblies as reference. Left table: ALLMAPS' orientation of assembled contigs based on markers' position on the genetic maps ("?" indicates a contig that was arbitrarily oriented); Right tables: Large (>1Mb) inversions detected by SyRI, and whether they are within an oriented ALLMAPS contig.

Supplemental Table S15. Summary of nucleotide sequence variants in core and noncore genes with potential consequences on coding sequence as identified by Variant Effect Predictor (VeP). SNPs and indels were analyzed separately. These values are shown in Figure 5. Predictions are based on annotations from the IT97K-499-35 genome assembly.

Figure 1. Principal component analysis of the UCR Minicore, indicating the accessions selected for sequencing and the subpopulation they belong to**.** Accessions in the plot are colored by the result of STRUCTURE for *K*=6, as shown in Muñoz-Amatriaín et al. (2021).

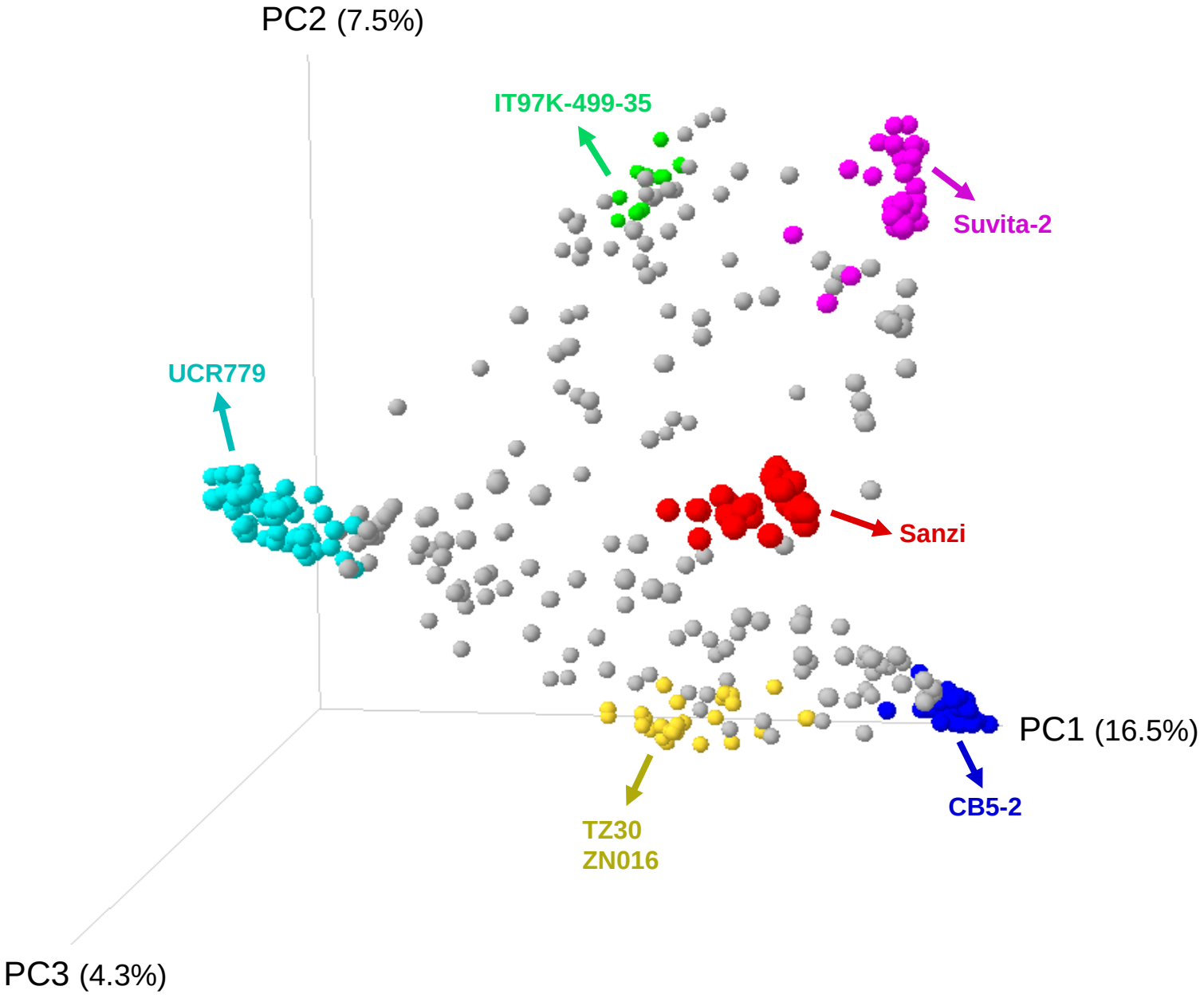

Figure 2. The number of genes identified in the pan-genome (pan-genes) and core genome (core genes) as new accessions are added.

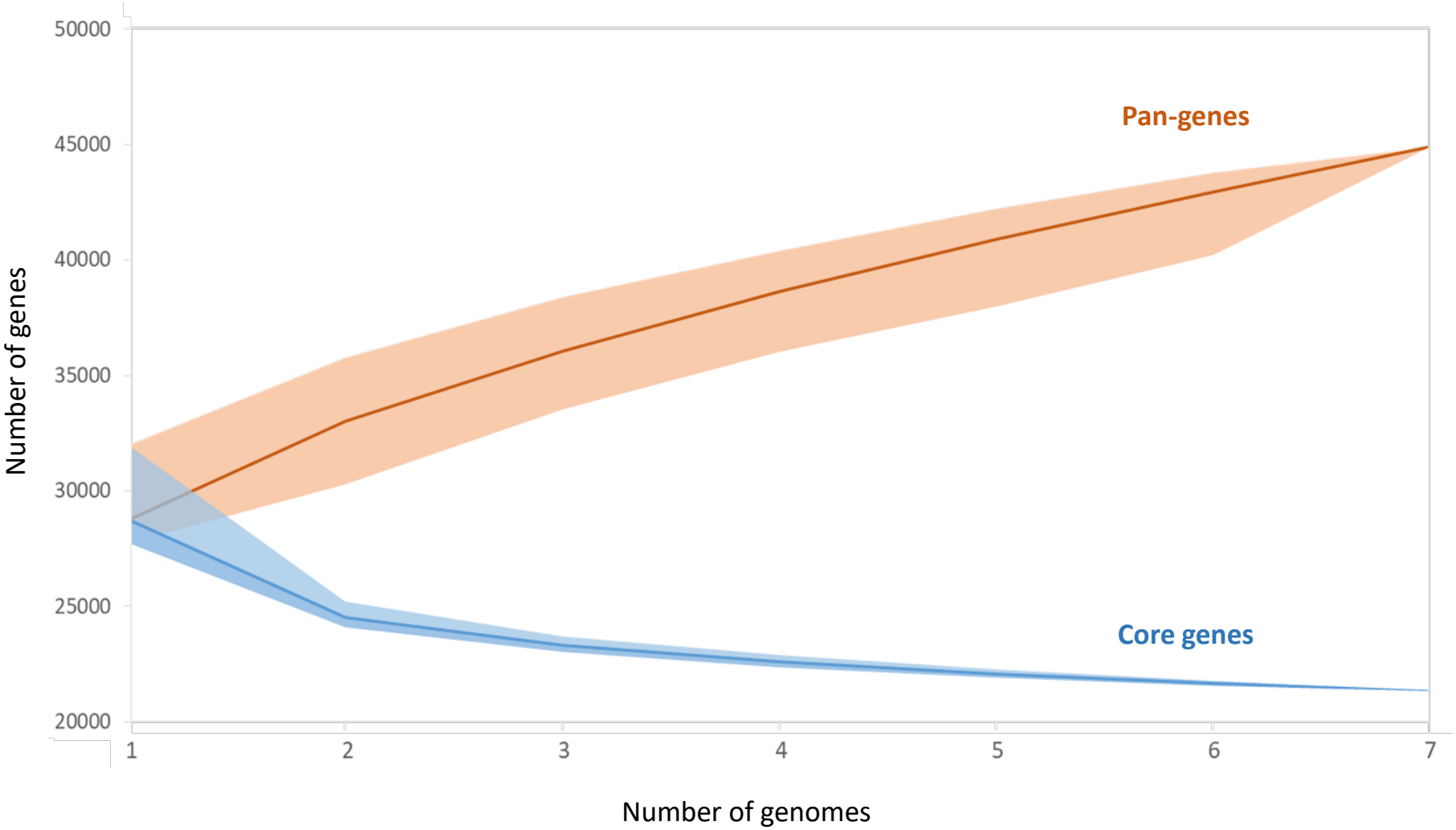

Figure 3. Gene Ontology (GO) term enrichment analysis. Significantly enriched GO terms for core (A) and noncore genes (B) are shown for GO-Slim categories belonging to Biological Process, Cellular Component, and Molecular Function aspects (in different colors). $-\log_{10}$ of FDR-adjusted p-values (q-values) are shown on the right of each bar.

A.

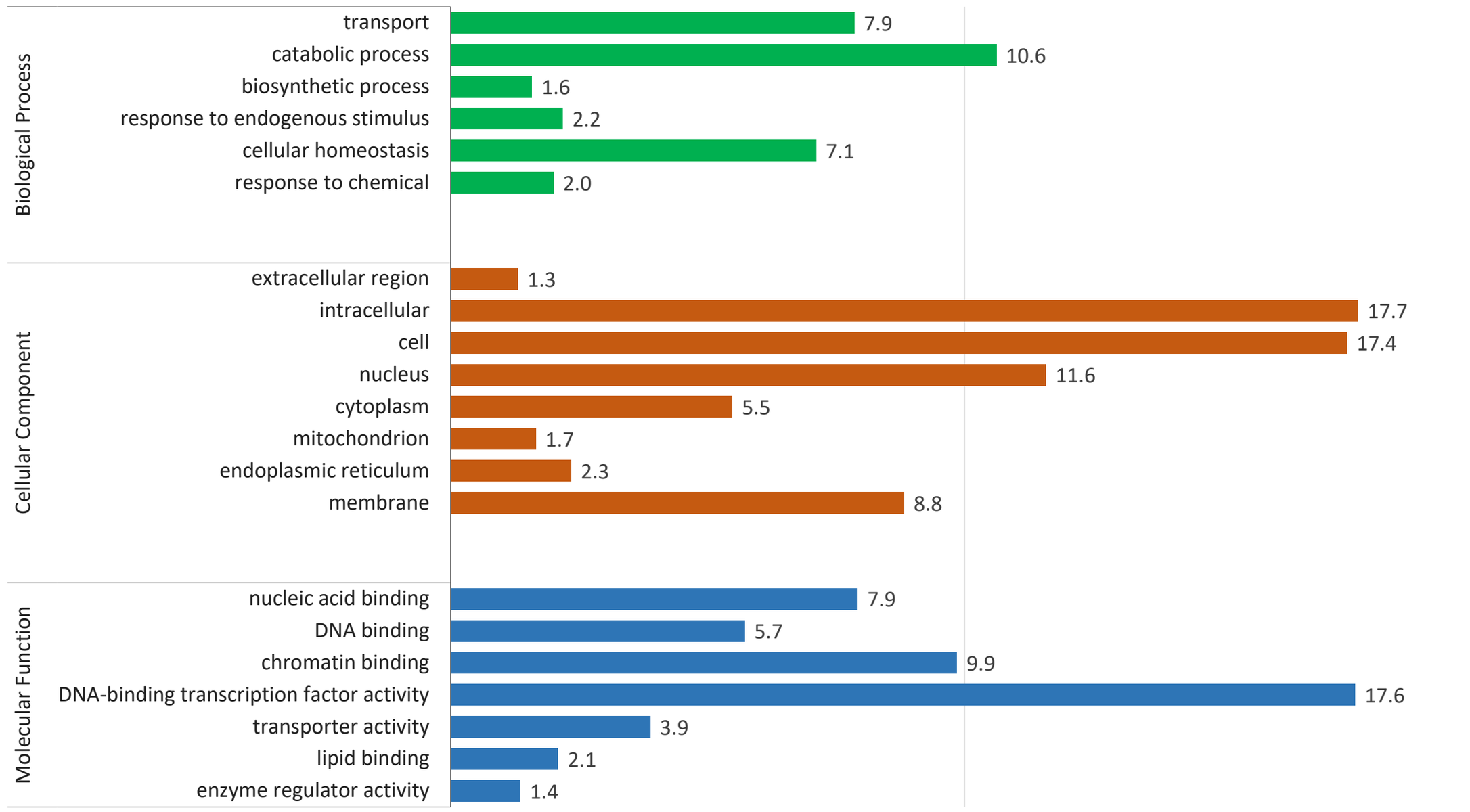

B.

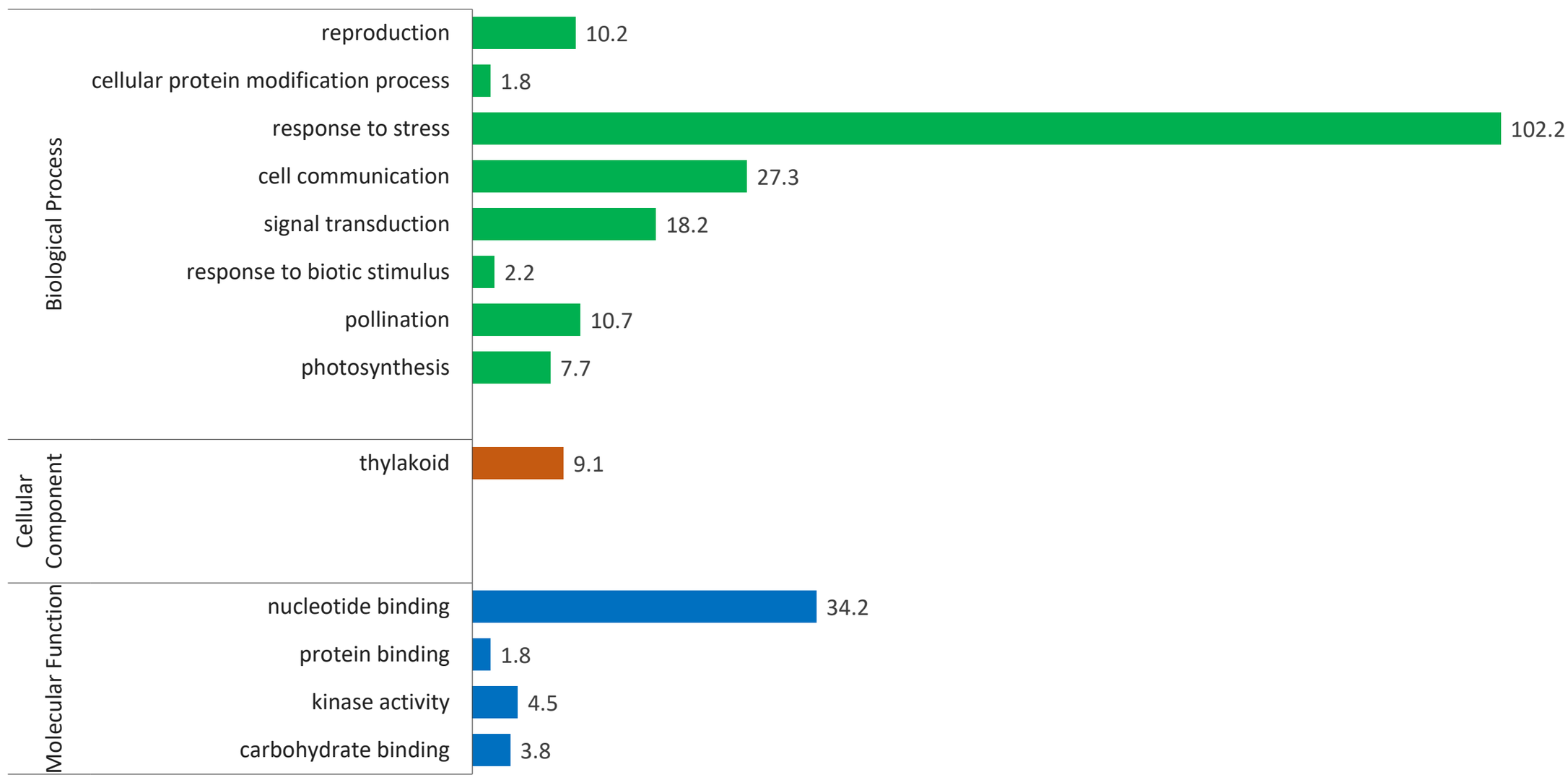

Figure 4. Representation of structural variations (of any size) detected by SyRI from the output of whole-genome pairwise alignments between the seven cowpea accessions. The black track indicates gene density in the reference genome IT97K-499-35, while the blue track indicates SNP density in the reference genome IT97K-499-35.

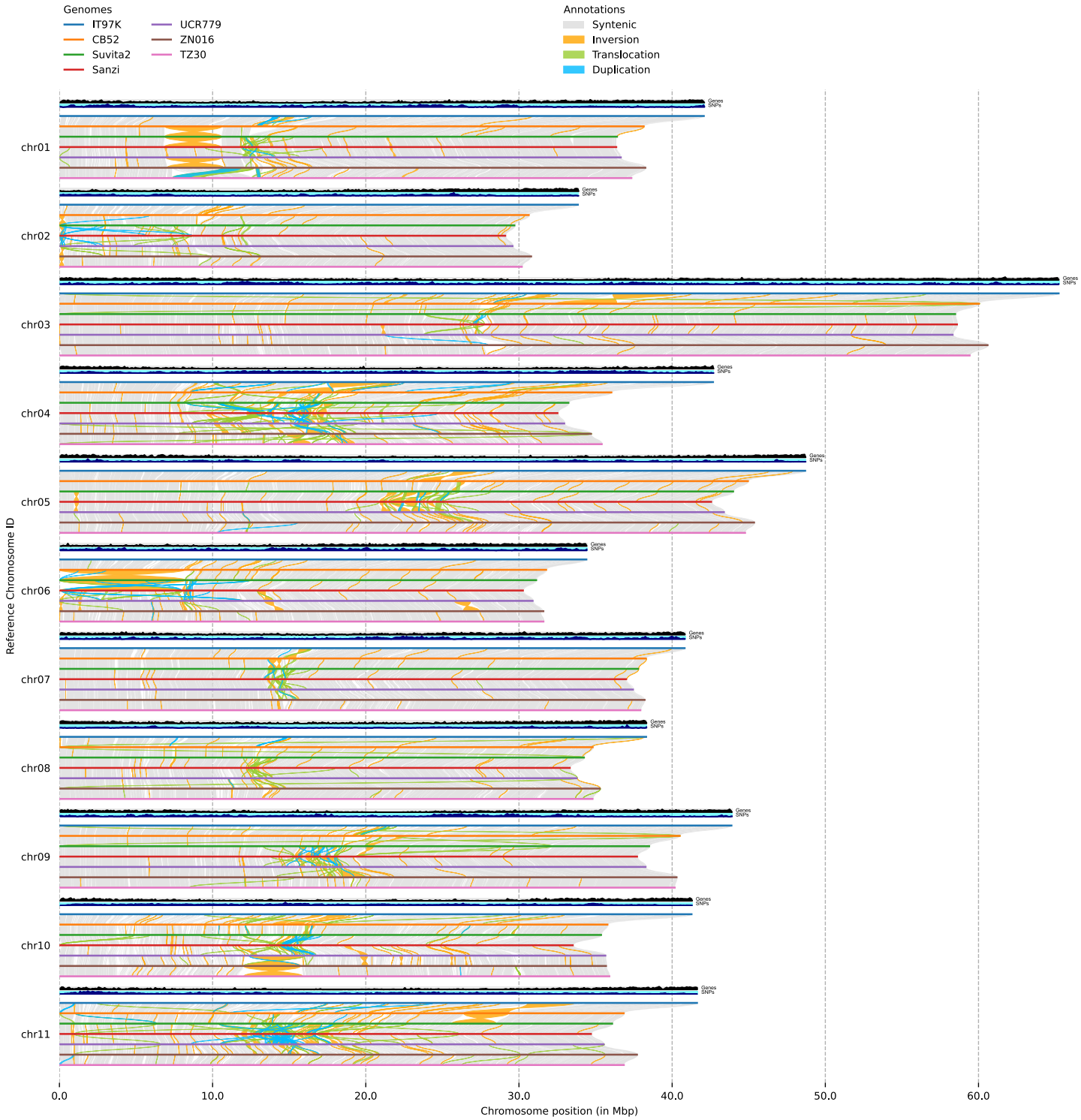

Figure 5. Variant effect predictor (VeP) annotations for SNPs and indels found in the core and noncore genes present in IT97K-499-35. Values on the y-axis are the absolute number of variants in each variant class.

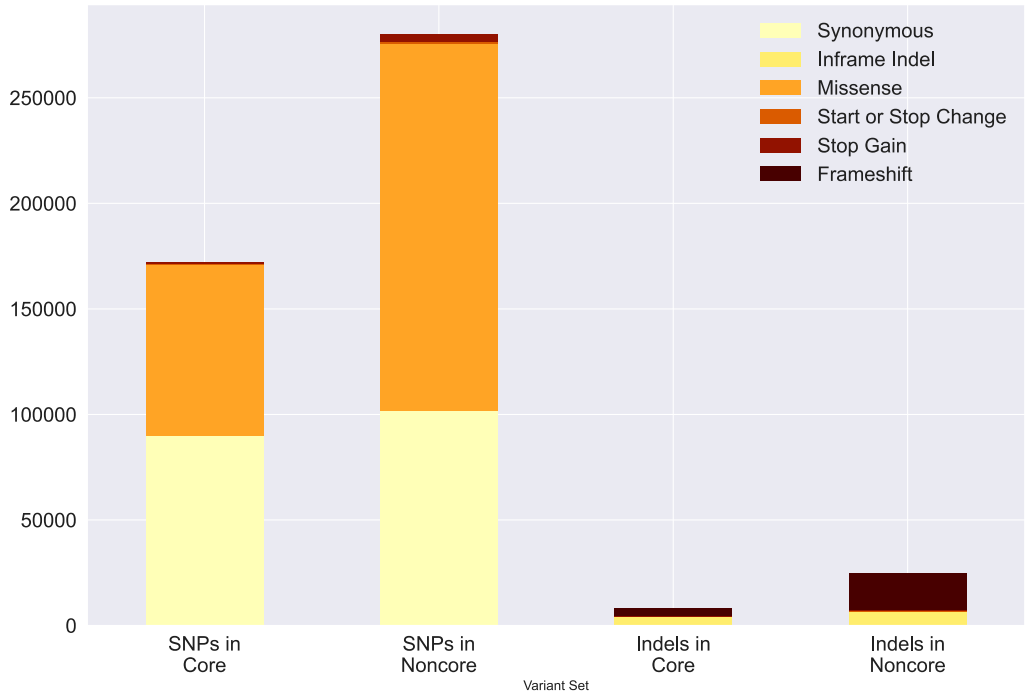

Figure 6A. Conservation of gene content within and across species. A region depicting gene content conservation and variability among cowpea genomes and other representative Phaseoleae species. Triangular glyphs represent order and orientation of genes, with color representing gene family memberships. (https://vigna.legumeinfo.org/tools/gcv).

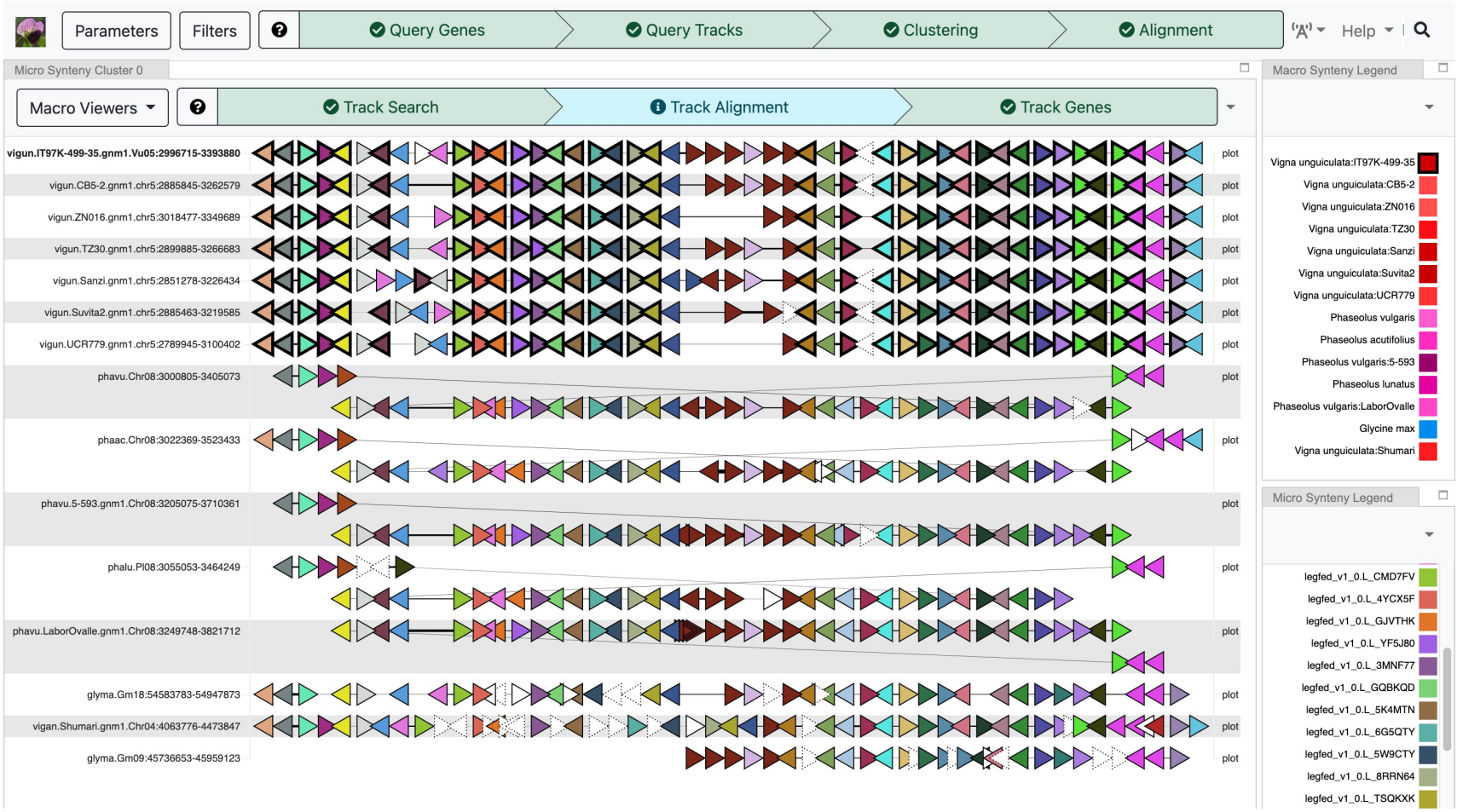

Figure 6B. Conservation of gene content within and across species. All cowpea proteins assigned to the family whose members exhibit copy number variation in Figure 6A are shown augmenting a dynamically recomputed gene tree at the Legume Information System, with genes from unanchored contigs not present in the chromosomes aligned in 6A indicated with arrows (https://mines.legumeinfo.org/cowpeamine).

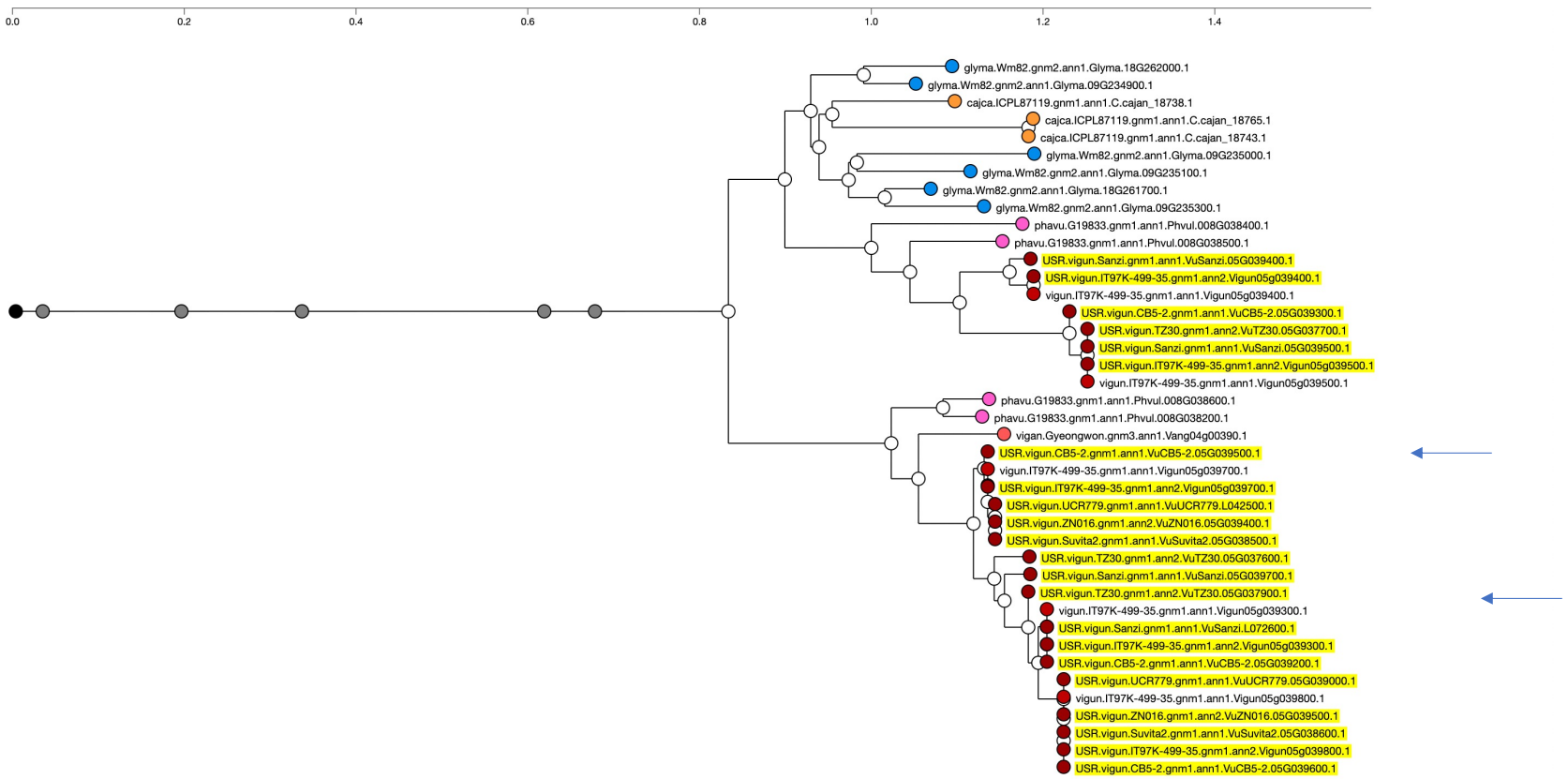

Table 1. Summary of assembly statistics, repetitive content, gene content and BUSCO4 completeness for the seven genomes.

	IT97K-499-35		CB5-2		Suvita-2		Sanzi		UCR779		ZN016		TZ30	
Assembly size (bp)	519,435,864		448,043,751		447,585,192		447,277,261		453,970,486		451,130,807		451,468,680	
N50 (bp)	41,684,185		36,897,245		36,142,647		34,759,918		35,700,653		37,764,243		36,906,789	
#Contigs/scaffolds	686		6,534		9,123		11,268		12,939		7,032		6,771	
#Contigs/scaffolds ≥ 100kbp	103		28		28		17		13		28		48	
#Contigs/scaffolds ≥ 1Mbp	13		11		11		11		11		11		11	
#Contigs/scaffolds ≥ 10Mp	11		11		11		11		11		11		11	
Longest contig (bp)	65,292,630		60,086,998		58,539,223		58,655,738		58,369,212		60,653,587		59,481,915	
Repetitive content	47.25%		45.52%		45.43%		45.50%		45.89%		45.68%		45.76%	
Annotated genes (#)	31,948		28,297		28,545		28,461		28,562		27,723		27,742	
BUSCO completeness														
Genome	1595	98.8%	1574	97.5%	1580	97.8%	1581	97.9%	1574	97.6%	1589	98.5%	1583	98.1%
Transcripts	1594	98.8%	1570	97.2%	1582	98.0%	1585	98.2%	1581	97.9%	1584	98.1%	1580	97.8%
Proteins	1595	98.8%	1569	97.3%	1584	98.2%	1587	98.3%	1585	98.2%	1584	98.1%	1582	98.0%

Table 2. Genomic coordinates of all inversions of size > 1 Mbp detected by comparing the seven cowpea genomes pairwise. IT97K-499-35 is abbreviated as IT97K.

	IT97K					
CB5-2	IT97K			CB5-2		
	chr03	36,118,990	40,333,678	chr03	32,390,474	36,391,036
	chr04	17,622,506	20,917,095	chr04	14,956,441	17,919,052
	chr05	25,746,455	27,269,915	chr05	23,493,794	24,846,894
	chr10	17,517,032	18,768,535	chr10	14,803,744	15,920,434
	chr11	30,575,673	33,619,557	chr11	26,382,727	29,314,033

	CB5-2					
Sanzi	IT97K			Sanzi		
	chr03	36,118,990	40,333,678	chr03	31,262,282	35,207,418
	chr04	17,944,012	20,826,275	chr04	13,863,317	16,451,333
	chr11	15,536,600	19,182,958	chr11	12,656,484	13,536,503

	CB5-2			Sanzi		
Suvita2	IT97K			Suvita2		
	chr01	7,882,945	11,829,903	chr01	6,880,499	10,585,839
	chr03	36,118,990	40,333,678	chr03	31,052,542	35,034,290
	chr04	17,620,322	21,043,166	chr04	14,040,335	16,532,009
	chr05	25,755,748	27,141,671	chr05	23,368,354	24,577,329
	chr06	15,232	8,928,750	chr06	105,004	8,215,985
	chr10	17,518,369	18,714,514	chr10	14,746,438	15,817,466

	CB5-2			Sanzi		
TZ30	IT97K			TZ30		
	chr01	8,078,984	11,774,887	chr01	7,037,437	12,547,938
	chr03	36,118,990	40,333,678	chr03	31,657,822	35,692,568
	chr04	21,097,140	22,121,274	chr04	17,439,719	18,187,637
	chr05	25,746,455	27,141,671	chr05	23,450,412	24,709,628
	chr06	28,973,468	30,151,695	chr06	26,590,042	27,712,655
	chr10	17,517,032	18,768,535	chr10	14,761,180	15,883,623

	CB5-2			Sanzi		
UCR779	IT97K			UCR779		
	chr03	36,119,072	40,333,678	chr03	30,810,075	34,783,649
	chr04	17,502,725	21,030,423	chr04	13,944,667	16,474,544
	chr05	25,746,455	27,075,873	chr05	22,985,675	24,003,974

	CB5-2			Sanzi		
ZN016	IT97K			ZN016		
	chr01	7,839,391	11,820,835	chr01	7,019,074	10,785,201
	chr03	36,118,990	40,333,678	chr03	32,843,668	36,858,590
	chr04	18,707,087	20,943,046	chr04	14,895,114	17,690,481
	chr05	25,746,455	27,223,043	chr05	24,265,392	25,383,012
	chr06	28,999,740	30,127,069	chr06	26,369,920	27,439,171
	chr10	14,534,255	18,390,632	chr10	12,350,844	15,751,259

	Sanzi			Suvita2		
Suvita2	CB5-2			Suvita2		
	chr01	6,882,777	10,598,583	chr01	6,880,226	10,585,839
	chr06	6,407	8,165,285	chr06	58,197	8,215,985
	chr11	26,392,061	29,309,384	chr11	25,612,417	28,506,945

	Sanzi			Suvita2		
TZ30	CB5-2			TZ30		
	chr01	7,073,895	10,598,703	chr01	6,952,274	12,533,400
	chr04	14,858,370	16,730,160	chr04	14,787,251	16,411,900
	chr06	26,597,860	27,660,154	chr06	26,590,042	27,686,349
	chr11	26,383,812	29,292,784	chr11	26,278,507	29,207,281

	Sanzi			Suvita2		
UCR779	CB5-2			UCR779		
	chr11	26,392,061	29,312,944	chr11	25,119,570	28,030,631

	Sanzi			Suvita2		
ZN016	CB5-2			ZN016		
	chr01	6,857,029	10,589,386	chr01	7,020,634	10,774,128
	chr04	16,349,146	17,910,419	chr04	16,191,362	17,334,982
	chr06	26,590,252	27,653,879	chr06	26,366,480	27,439,152
	chr10	12,100,642	15,920,434	chr10	12,026,103	15,751,269
	chr11	26,357,807	29,309,414	chr11	27,061,318	30,061,182

	Suvita2			TZ30		
TZ30	Suvita2			TZ30		
	chr01	7,006,278	10,479,491	chr01	7,037,894	12,533,400
	chr06	25,185,327	26,275,534	chr06	26,599,616	27,728,577

	Suvita2			TZ30		
UCR779	Suvita2			UCR779		
	chr01	6,890,035	10,585,839	chr01	6,931,327	10,601,930
	chr06	110,090	8,055,043	chr06	25,279	8,037,739

	Suvita2			TZ30		
ZN016	Suvita2			ZN016		
	chr01	6,813,588	10,522,595	chr01	7,020,980	10,775,930
	chr06	25,198,638	26,275,534	chr06	26,369,920	27,460,156
	chr10	11,712,476	14,725,119	chr10	12,070,488	15,606,154

	TZ30			UCR779		
UCR779	TZ30			UCR779		
	chr01	7,037,894	12,536,905	chr01	7,105,707	10,558,424
	chr04	14,846,045	16,411,900	chr04	13,944,667	15,345,835
	chr06	26,590,042	27,686,706	chr06	25,789,928	26,854,548

	TZ30			ZN016		
ZN016	TZ30			ZN016		
	chr04	15,234,860	16,411,900	chr04	14,817,248	15,900,761
	chr10	12,029,208	15,883,623	chr10	12,026,103	15,749,232

	UCR779			ZN016		
ZN016	UCR779			ZN016		
	chr01	6,946,955	10,601,930	chr01	7,020,634	10,728,684
	chr06	25,789,928	26,848,252	chr06	26,369,920	27,427,414
	chr10	12,451,287	15,886,883	chr10	12,177,925	15,742,142